J. Fluid Mech. (1994), *vol.* 268, *pp.* 231–265

Local fluid and heat flow near contact lines

By D. M. ANDERSON† AND S. H. DAVIS

Department of Engineering Sciences and Applied Mathematics, Northwestern University, Evanston, IL 60208, USA

(Received 20 August 1993 and in revised form 30 November 1993)

We consider steady two-dimensional fluid flow and heat transfer near contact lines in single-phase and two-phase systems. Both single- and double-wedge geometries admit separable solutions in plane polar coordinates for both thermal and flow fields. We consider the class of functions which have bounded temperatures and velocities at the corner. When free surfaces are present, we seek *local solutions*, those that satisfy all local boundary conditions, and *partial local solutions*, those that satisfy all but the normal-stress boundary condition. Our aim in this work is to describe local fluid and heat flow in problems where these fields are coupled by determining for which wedge angles solutions exist, identifying singularities in the heat flux and stress which are present at contact lines, and determining the dependence of these singularities on the wedge angles. For thermal fields in two phases we identify two modes of heat transfer that are analogous to the two modes identified by Proudman & Asadullah (1988) for two-fluid flow. For non-isothermal flow, locally, convection does not play a role but coupling through thermocapillary effects on non-isothermal free surfaces can arise. We find that under non-isothermal conditions a planar free surface must leave a planar rigid boundary at an angle of π, the same angle found by Michael (1958) for an isothermal rigid/free wedge, in order to satisfy all local boundary conditions. Finally, we find that situations arise where no coupled solutions of the form sought can be found; we discuss means by which alternative solutions can be obtained.

1. Introduction

Corner flows are often present under non-isothermal conditions in which case both fluid flow and heat transfer are simultaneously acting (e.g. non-isothermal flow in a driven cavity (Burggraf 1966), or thermocapillary-driven flow in a box (Zebib, Homsy & Meiburg 1985)). Moving-contact-line problems can be in this category (e.g. droplets spreading on heated substrates (Ehrhard & Davis 1991)). Further, such situations always occur at the 'edges' of fronts that define phase transformation. For example, if a droplet of volatile liquid spreads on a heated surface, the evaporative mass loss near the contact line modifies the local flow (Anderson 1993). Contact lines joining multiple-phase/multiple-field regions occur frequently in crystal growth systems. Meniscus-defined processes such as float-zone, and Czochralski systems, as well as other solidification processes are in this category (e.g. see Brown 1988).

Two-dimensional isothermal viscous flow in a corner region has been studied by several authors. Dean & Montagnon (1949) considered a wedge bounded by two rigid planes and determined properties of the flow as functions of the wedge angle. Michael (1958) considered the same geometry but with one solid boundary and one free surface

† Present address: Department of Applied Mathematics and Theoretical Physics, University of Cambridge, Silver Street, Cambridge CB3 9EW, UK.

and found that in order for the free surface to be stress-free the wedge angle must be π. Moffatt (1964) considered these cases as well as the case of a wedge bounded by two free surfaces and described in detail situations in which sequences of eddies, now known as Moffatt vortices, can be present in the flow. Proudman & Asadullah (1988) considered two-fluid systems where the fluids meet along a flat surface. They identified two modes of flow in the limit of small viscosity ratio. The first of these modes, the 'velocity' mode, is that obtained by a single-phase analysis. The second, the 'stress' mode, is a new mode resulting from a second phase with small viscosity. Anderson & Davis (1993) considered two-fluid isothermal flow in a wedge bounded by two rigid planes of arbitrary angle. They identified singularities in the flow, Moffatt vortices, as well as geometries consistent with separable local solutions. They showed that the two modes identified by Proudman & Asadullah (1988) were present for all wedge angles.

The goal of the present work is to extend the isothermal corner flow results to cases of non-isothermal flow near contact lines occurring in single-phase and two-phase systems. In §§2.1 and 2.2 we shall look at heat transfer and non-isothermal fluid flow in a single phase. Here we find that the thermal and flow fields are locally coupled only through thermocapillarity on non-isothermal free surfaces. We also find that situations arise where no coupled solutions of the form sought can be found; means by which alternative solutions can be found are discussed in §5. In §3 we shall consider these fields in two phases. Here we first consider two-phase pure heat transfer (§3.1) and identify two modes of heat transfer in the limit of large or small conductivity ratio; these two modes are analogous to the two modes of flow identified by Proudman & Asadullah (1988) for two-fluid flow in the limit of vanishing viscosity ratio. For non-isothermal flow (§3.2) we find that a planar free surface must leave a planar rigid boundary at an angle of π, the same angle found by Michael (1958) for a planar free surface and a planar rigid boundary under isothermal conditions. In §4 we examine non-isothermal flow using a small-capillary-number expansion, and compare the results with the isothermal results found by Anderson & Davis (1993). As with single-phase non-isothermal flow, we find situations where no coupled solutions of the form sought can be found and discuss interpretations and alternative approaches in §5.

We shall consider the class of solutions that have bounded temperatures and velocities at the wedge vertex. We shall seek both *local solutions*, those that satisfy *all* local boundary conditions, and *partial local solutions*, those that, when free surfaces are present, satisfy all local boundary conditions with the exception of the normal-stress boundary condition. Partial local solutions are important in the description of the local flow valid for infinite surface tension (or zero capillary number). When perturbation methods for small capillary number are used, conditions on the flow imposed by the normal-stress boundary condition do not appear in the leading-order problem and therefore partial local solutions can be viewed as leading-order solutions for these cases. Partial local solutions also describe cases in which there exists an appropriate spatially varying pressure distribution outside the free surface such that the normal-stress boundary condition is satisfied without further restriction on the flow (Moffatt 1964). Under such an assumption, the restriction of small capillary number is not necessary. When such provisions are made for the pressure, these solutions satisfy all local boundary conditions and can be thought of as specialized local solutions.

$\theta = 0$	$\theta = \alpha$
nf	nf
ft	nf
ft	ft

TABLE 1. Types of thermodynamic boundary conditions for a single wedge

2. Single-phase systems

2.1. *Thermal field*

Consider steady two-dimensional heat transfer in a wedge. The wedge of material, solid or fluid, has boundaries at $\theta = 0$ and $\theta = \alpha$ where θ is the azimuthal angle. The radial distance from the corner is r. In the case of a fluid wedge, heat transfer is in general coupled to the flow through the advection term $\boldsymbol{u}\cdot\nabla T$ in the energy equation. In the steady state this reduces to $\nabla^2 T = 0$ when

$$r \ll \mathscr{K}^{th}/U, \tag{2.1}$$

where $\mathscr{K}^{th}$ is the thermal diffusivity and U is a velocity scale. Note that when the corner is a flat free surface, for example, the existence of such a region is not guaranteed. In the case of a wedge of solid material this equation is exact.

The general thermal boundary condition is $k(\hat{\boldsymbol{n}}\cdot\nabla T) = -h(T - T_W)$, where $\hat{\boldsymbol{n}}$ is a unit normal directed out of the wedge, T_W is the far-field temperature of the boundary material, k is the thermal conductivity, and h is the heat transfer coefficient. In polar coordinates for a wedge this becomes

$$\pm\frac{k}{r}\frac{\partial T}{\partial\theta} = h(T - T_W). \tag{2.2}$$

If the boundary material is a perfect conductor (i.e. $h = \infty$) then this condition reduces to $T = T_W$. If the boundary material is a perfect insulator (i.e. $h = 0$) then $\partial T/\partial\theta = 0$ (i.e. zero heat flux). It can be shown that the general boundary condition (2.2) gives the same leading-order behaviour near the corner when $h \neq \infty$ as the no-flux case. Therefore, in what follows, we shall consider just two types of boundary conditions. The different combinations are summarized in table 1. Here 'nf' refers to the no-flux condition

$$\frac{\partial T}{\partial\theta} = 0 \tag{2.3}$$

and 'ft' refers to the fixed temperature condition

$$T = T_W. \tag{2.4}$$

In each case we seek separable solutions to Laplace's equation of the form

$$T(r,\theta) = r^{\tau}[A^{th}\cos\tau\theta + B^{th}\sin\tau\theta] + C^{th}\theta + D^{th}. \tag{2.5}$$

Here, τ is the separation constant taken to be positive (negative values of τ, as well as $\ln r$ terms, although solutions to Laplace's equation, give rise to unbounded temperatures at the origin and therefore are excluded from the present analysis). This form of the solution allows one to examine directly through the value of the exponent, τ, singularities at the corner. These results are summarized as follows:

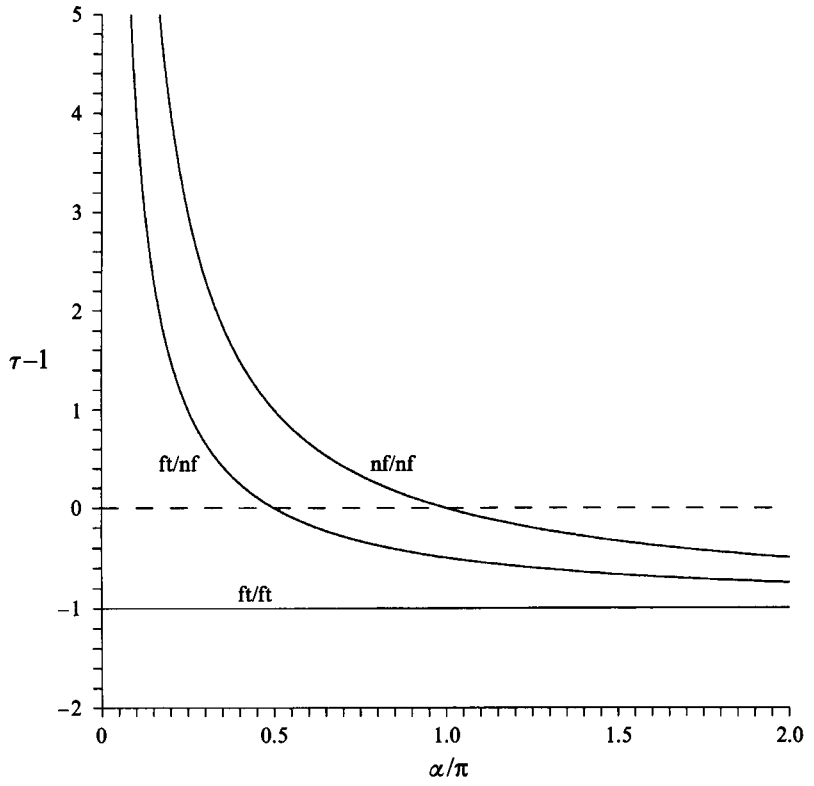

FIGURE 1. Single-phase pure heat transfer: the smallest heat-flux exponent, $\tau-1$, for three different types of thermal boundary conditions: no-flux/no-flux (nf/nf), fixed-temperature/no-flux (ft/nf), and fixed-temperature/fixed-temperature (ft/ft). The heat flux becomes singular when $\tau-1$ becomes negative. Notice that the heat flux in the ft/ft case, which has a $(1/r)$ behaviour due to the differing boundary data on the two wedge boundaries, is the most singular while the nf/nf case is the least singular. Note that τ is real.

(a) two perfect insulators ($\partial T/\partial\theta = 0$ on $\theta = 0, \alpha$)

$$T = D^{th} + A_m^{th} r^\tau \cos\tau\theta, \quad \tau = m\pi/\alpha, \quad m = 1, 2, 3, \ldots; \tag{2.6}$$

(b) one perfect conductor and one perfect insulator ($T = T_0$ on $\theta = 0$ and $\partial T/\partial\theta = 0$ on $\theta = \alpha$)

$$T = T_0 + B_m^{th} r^\tau \sin\tau\theta, \quad \tau = (m+\tfrac{1}{2})\pi/\alpha, \quad m = 0, 1, 2, \ldots; \tag{2.7}$$

(c) two perfect conductors ($T = T_0$ on $\theta = 0$ and $T = T_\alpha$ on $\theta = \alpha$)

$$T = T_0 + (T_\alpha - T_0)\theta/\alpha + B_m^{th} r^\tau \sin\tau\theta, \quad \tau = m\pi/\alpha, \quad m = 1, 2, 3, \ldots. \tag{2.8}$$

From (2.5) we find that the heat flux in both radial and azimuthal directions, in general, is proportional to $r^{\tau-1}$. Figure 1 shows a plot of the heat flux exponents, $\tau-1$, and indicates the nature of the heat flux at the origin. When $\tau-1 < 0$ the heat flux is singular; otherwise it is non-singular. Note that τ is always real. In case (a), the heat flux is singular for $\alpha > \pi$ but is always integrable. In case (b), the heat flux is singular for $\alpha > \frac{1}{2}\pi$ but always integrable. The heat flux in case (c) is singular and non-integrable for all wedge angles whenever $T_0 \neq T_\alpha$ which reflects the discontinuous boundary data at the vertex. If $T_0 = T_\alpha$ the r^{-1} singularity is relieved and the description of the singularities is the same as in case (a). Notice that the nf/nf case, case (a), is the 'least' singular while the ft/ft case, case (c), is the 'most' singular. We find that larger wedge angles correspond to stronger heat flux singularities and that $\tau \to \infty$ as $\alpha \to 0$.

2.2. *Non-isothermal flow*

2.2.1. *Preliminaries*

In this section we describe the general formulation for non-isothermal fluid flow in a single wedge. We seek separable solutions for both the thermal and flow fields. For a local description of the flow as Stokes flow, we require that $r \ll \nu/U$, where ν is the kinematic viscosity, and U is a velocity scale. For the thermal problem, there is a similar restriction on r given by (2.1). Therefore, for $r \ll \min(\nu/U, \mathscr{K}^{th}/U)$ the equations governing non-isothermal flow are $\nabla^2\psi = 0$ and $\nabla^2 T = 0$. Here ψ is the streamfunction and is related to the velocity vector, $\boldsymbol{u}$, in polar coordinates by

$$\boldsymbol{u} = \left(\frac{1}{r}\frac{\partial\psi}{\partial\theta}, -\frac{\partial\psi}{\partial r}\right). \tag{2.9}$$

As a result, there is no coupling in the bulk and hence any local coupling must arise at the boundaries.

When a free surface is present, variations in surface tension arise from temperature variations along the free surface; these surface-tension gradients drive the flow. In the following analysis we assume that the surface tension varies linearly with temperature and is given by $\gamma = \gamma_0 - \gamma'(T - T_0)$ where γ_0 is the surface tension at the reference temperature T_0 and γ' is constant and positive; thus $\gamma' = |\mathrm{d}\sigma/\mathrm{d}T|$. This gives the thermocapillary condition

$$[\boldsymbol{\sigma}\cdot\hat{\boldsymbol{n}}]\cdot\hat{\boldsymbol{t}} = -\gamma'(\hat{\boldsymbol{t}}\cdot\boldsymbol{\nabla})\,T, \tag{2.10}$$

where $\boldsymbol{\sigma} = -p\boldsymbol{I} + \mu[\boldsymbol{\nabla u} + (\boldsymbol{\nabla u})^T]$ is the stress tensor with pressure p. Note that for wedges bounded by two rigid surfaces, for cases where $\gamma' = 0$, or for cases with isothermal free surfaces, the thermal and flow fields are locally decoupled and the solutions are given by the superposition of the results for pure heat transfer and the results for isothermal flow (e.g. see Anderson & Davis 1993).

Even with thermocapillarity present, the thermal problem remains unchanged from the single-phase pure heat transfer problem and decouples from the flow. The thermal fields are, in fact, just the single-phase thermal fields of §2.1.

When thermocapillarity is present, the differential system for the flow changes from a homogeneous one (i.e. isothermal flow) to an inhomogeneous one (i.e. non-isothermal flow) since the flow has a component that is locally driven. Recall that in pure-heat-transfer problems we found eigenvalues $\tau(\alpha)$ which allowed non-trivial thermal fields (see figure 1). Hence in order to balance forces on the free surface near the corner, the streamfunction must have terms proportional to $r^{\tau+1}$ corresponding to a non-zero shear stress generated by the temperature gradients. Therefore, the form of the streamfunction is given by

$$\begin{aligned}\psi_p = {} & r^{\tau+1}[A_\tau\cos(\tau+1)\theta + B_\tau\sin(\tau+1)\theta + C_\tau\cos(\tau-1)\theta + D_\tau\sin(\tau-1)\theta] \\ & + r^2(A_1\cos 2\theta + B_1\sin 2\theta + C_1\theta + D_1) \\ & + r(A_0\cos\theta + B_0\sin\theta + C_0\theta\cos\theta + D_0\theta\sin\theta),\end{aligned} \tag{2.11}$$

where A_i, B_i, C_i, D_i for $i = 0, 1, \tau$ are unknown constants to be determined by the boundary conditions.

The isothermal-flow result, which corresponds to zero shear stress on the free surface, is still a complementary solution and must be superposed on the particular solution for a complete description of the local flow. The isothermal-flow problem has eigenvalues $\sigma(\alpha)$, corresponding to the power of r in the flow solution, analogous to the

temperature exponent, τ. These eigenvalues, $\sigma(\alpha)$, for which nontrivial flow could be obtained are given by

$$\sigma \sin\alpha \pm \sin\sigma\alpha = 0 \tag{2.12}$$

for a rigid/rigid wedge (Dean & Montagnon 1949),

$$\sigma \sin 2\alpha - \sin 2\sigma\alpha = 0 \tag{2.13}$$

for partial local solutions for a rigid/free wedge (Moffatt 1964), and

$$\sin(\sigma-1)\alpha \sin(\sigma+1)\alpha = 0 \tag{2.14}$$

for partial local solutions for a free/free wedge (Moffatt 1964; Anderson & Davis 1993).

For the terms proportional to r^2 in the streamfunction there are similar eigenvalues (for special angles). These are given by

$$\sin\alpha(\sin\alpha - \alpha\cos\alpha) = 0 \tag{2.15}$$

for a rigid/rigid wedge,

$$\sin 2\alpha - 2\alpha\cos 2\alpha = 0 \tag{2.16}$$

for partial local solutions for a rigid/free wedge, and

$$\sin 2\alpha = 0 \tag{2.17}$$

for partial local solutions for a free/free wedge (see Anderson & Davis 1993). Therefore, the complete local streamfunction will have terms proportional to $r^{\tau+1}$ as well as $r^{\sigma+1}$, r^2 and r as allowed by the appropriate isothermal flow.

Of particular interest will be the comparison of the exponents σ and τ. Notice that if τ corresponds to an eigenvalue of the isothermal problem (i.e. $\tau(\alpha) = \sigma(\alpha)$ for some α), there will be a solvability condition required on the forcing terms. We shall find that in some cases this solvability condition cannot be satisfied unless $\gamma' = 0$ or unless the temperature field is uniform throughout the wedge; this implies that the solution to the problem, as posed, with $\gamma' \neq 0$ requires an isothermal corner. Further interpretations in these cases are given in §5.

Since the thermal problem decouples from the flow and $T \sim r^{\tau} f_{\tau}(\theta)$, we know that the surface temperature gradients have the form

$$\frac{\partial T}{\partial r} \sim \tau r^{\tau-1} f_{\tau}(\theta). \tag{2.18}$$

Therefore we can solve the flow problem for the rigid/free wedge case and for the free/free wedge case which hold for general values of τ and general thermal boundary conditions. We can then apply these general results to specific thermal fields by substituting appropriate values of τ and $f_{\tau}(\theta)$.

Rigid/free wedge: The hydrodynamic boundary conditions are given by

$$\psi = \frac{\partial\psi}{\partial\theta} = 0 \qquad \text{on} \quad \theta = 0, \tag{2.19a}$$

$$\psi = 0 \qquad \text{on} \quad \theta = \alpha, \tag{2.19b}$$

$$\mu \frac{1}{r^2}\frac{\partial^2\psi}{\partial\theta^2} = -\tau\gamma'_{\alpha} f_{\tau}(\alpha) r^{\tau-1} \qquad \text{on} \quad \theta = \alpha, \tag{2.19c}$$

$$-p + \frac{2\mu}{r}\left(\frac{1}{r}\frac{\partial\psi}{\partial\theta} - \frac{\partial^2\psi}{\partial r\,\partial\theta}\right) = 0 \qquad \text{on} \quad \theta = \alpha. \tag{2.19d}$$

Here μ is the viscosity and γ'_α refers to $|\mathrm{d}\gamma/\mathrm{d}T|$ evaluated on $\theta = \alpha$. The pressure, p, is related to ψ through the Stokes equations. The thermocapillary condition requires that $\psi \sim r^{\tau+1}$. We distinguish between cases where $\tau \neq 1$ and those with $\tau = 1$ since these two cases require different forms of the streamfunction (see (2.11)). In the following description we classify solutions according to the value of τ, which is determined by the thermal problem. Only the particular solution, ψ_p, is given; however, the complete local description of the flow requires the homogeneous, or isothermal, contribution as well. We seek both local solutions, ψ_p and partial local solutions, $\tilde{\psi}_p$.

The solutions can be categorized as follows: (1i) $\tau \neq 1$, $\tau \sin 2\alpha - \sin 2\tau\alpha \neq 0$; (1ii) $\tau \neq 1$, $\tau \sin 2\alpha - \sin 2\tau\alpha = 0$; (2i) $\tau = 1$, $\sin 2\alpha - 2\alpha \cos 2\alpha \neq 0$; and (2ii) $\tau = 1$, $\sin 2\alpha - 2\alpha \cos 2\alpha = 0$. Essentially we distinguish between cases in which τ corresponds to an eigenvalue of the homogeneous problem (cases (1ii) and (2ii)) and those in which it does not (cases (1i) and (2i)).

(1i) When $\tau \neq 1$ and $\tau \sin 2\alpha - \sin 2\tau\alpha \neq 0$, partial local solutions are given by

$$\tilde{\psi}_p = -\frac{\gamma'_\alpha f_\tau(\alpha)\, r^{\tau+1}}{\mu(\tau \sin 2\alpha - \sin 2\tau\alpha)} g(\theta, \alpha, \tau), \tag{2.20}$$

where $g(\theta, \alpha, \tau)$ is given by

$$\frac{g(\theta, \alpha, \tau)}{\sin \tau\alpha \sin \alpha} \equiv \frac{\sin(\alpha - \theta)}{\sin \alpha} \sin \tau\theta - \frac{\sin \tau(\alpha - \theta)}{\sin \tau\alpha} \tau \sin \theta. \tag{2.21}$$

Local solutions are found only for $\alpha = \pi$ and are given by

$$\psi = \frac{\gamma'_\alpha f_\tau(\pi)\, r^{\tau+1}}{2\mu \cos \tau\pi} \sin \tau\theta \sin \theta. \tag{2.22}$$

We immediately see that form (2.20) breaks down when τ corresponds to an eigenvalue of the isothermal flow problem (i.e. when $\tau \sin 2\alpha - \sin 2\tau\alpha = 0$).

(1ii) When $\tau \neq 1$ and $\tau \sin 2\alpha - \sin 2\tau\alpha = 0$, there is a solvability condition on the right-hand-side forcing in (2.19). For these values of τ no non-zero local or partial local solutions exist unless $\alpha = \pi$ and $\tau = 2, 3, 4, \ldots$. In this case both local and partial local solutions have the same form (i.e. the normal-stress boundary condition is identically satisfied by the partial local solution form), given by

$$\psi_p = \tilde{\psi}_p = \frac{\gamma'_\alpha}{2\mu}(-1)^\tau f_\tau(\pi)\, r^{\tau+1} \sin \tau\theta \sin \theta. \tag{2.23}$$

(2i) When $\tau = 1$ and $\sin 2\alpha - 2\alpha \cos 2\alpha \neq 0$, partial local solutions are given by

$$\tilde{\psi}_p = -\frac{\gamma'_\alpha f_1(\alpha)\, r^2}{4\mu(\sin 2\alpha - 2\alpha \cos 2\alpha)} \times [(2\alpha - \sin 2\alpha)(\cos 2\theta - 1) - (\cos 2\alpha - 1)(2\theta - \sin 2\theta)]. \tag{2.24}$$

Again we see that this solution breaks down when $\sin 2\alpha - 2\alpha \cos 2\alpha = 0$, (i.e. (2.16)). Local solutions exist only when $\alpha = \pi$ and are given by

$$\psi_p = -\frac{\gamma'_\alpha}{4\mu} f_1(\pi)\, r^2 (1 - \cos 2\theta). \tag{2.25}$$

(2ii) When $\tau = 1$ and $\sin 2\alpha - 2\alpha\cos 2\alpha = 0$, no non-trivial streamfunctions exist.

Free/free wedge: Here thermocapillary effects may be present on both boundaries. The hydrodynamic boundary conditions are given by

$$\psi = 0 \qquad \text{on} \quad \theta = 0, \alpha, \tag{2.26a}$$

$$\frac{\mu}{r^2}\frac{\partial^2\psi}{\partial\theta^2} = \tau\gamma_0' f_\tau(0)\, r^{\tau-1} \qquad \text{on} \quad \theta = 0, \tag{2.26b}$$

$$\frac{\mu}{r^2}\frac{\partial^2\psi}{\partial\theta^2} = -\tau\gamma_\alpha' f_\tau(\alpha)\, r^{\tau-1} \qquad \text{on} \quad \theta = \alpha, \tag{2.26c}$$

$$-p + \frac{2\mu}{r}\left(\frac{1}{r}\frac{\partial\psi}{\partial\theta} - \frac{\partial^2\psi}{\partial r\,\partial\theta}\right) = 0 \qquad \text{on} \quad \theta = 0, \alpha. \tag{2.26d}$$

Note that γ_0' and γ_α' are not necessarily equal. These boundary conditions require $\psi \sim r^{\tau+1}$.

Again the solutions can be categorized into resonant and non-resonant cases: (3i) $\tau \neq 1$, $\sin(\tau+1)\alpha \sin(\tau-1)\alpha \neq 0$; (3ii) $\tau \neq 1$, $\sin(\tau \pm 1)\alpha = 0$, $\sin(\tau \mp 1)\alpha \neq 0$; (3iii) $\tau \neq 1$, $\sin(\tau+1)\alpha = \sin(\tau-1)\alpha = 0$; (4i) $\tau = 1$, $\sin 2\alpha \neq 0$; and (4ii) $\tau = 1$, $\sin 2\alpha = 0$. Note that cases (3ii), (3iii), and (4ii) are the resonant cases in which τ corresponds to an eigenvalue of the homogeneous problem.

(3i) When $\tau \neq 1$ and $\sin(\tau+1)\alpha \sin(\tau-1)\alpha \neq 0$, partial local solutions are given by

$$\tilde{\psi}_p = \frac{r^{\tau+1}}{2\mu}\left[\gamma_0' f_\tau(0)\sin\tau\theta\sin\theta + \tfrac{1}{2}(\gamma_\alpha' f_\tau(\alpha) + \gamma_0' f_\tau(0)\cos(\tau+1)\alpha)\frac{\sin(\tau+1)\theta}{\sin(\tau+1)\alpha}\right.$$
$$\left. -\tfrac{1}{2}(\gamma_\alpha' f_\tau(\alpha) + \gamma_0' f_\tau(0)\cos(\tau-1)\alpha)\frac{\sin(\tau-1)\theta}{\sin(\tau-1)\alpha}\right]. \tag{2.27}$$

Local solutions are given by

$$\psi_p = \frac{r^{\tau+1}}{2\mu}\left[\gamma_0' f_\tau(0)\sin\tau\theta\sin\theta + \frac{\gamma_\alpha' f_\tau(\alpha) + \gamma_0' f_\tau(0)\cos(\tau+1)\alpha}{\sin(\tau+1)\alpha}\cos\tau\theta\sin\theta\right] \tag{2.28}$$

subject to the constraints

$$\sin\alpha[\gamma_0' f_\tau(0)\cos\alpha + \gamma_\alpha' f_\tau(\alpha)\cos\tau\alpha] = 0, \tag{2.29a}$$

$$\sin\alpha[\gamma_0' f_\tau(0)\sin\alpha + \gamma_\alpha' f_\tau(\alpha)\sin\tau\alpha] = 0. \tag{2.29b}$$

(3ii) When $\tau \neq 1$ and $\sin(\tau \pm 1)\alpha = 0$ but $\sin(\tau \mp 1)\alpha \neq 0$ (i.e. $\sin 2\alpha \neq 0$, and $\tau = m\pi/\alpha - 1$ where m is any integer such that $\tau > 0$), we find that no non-trivial solutions exist unless

$$\gamma_\alpha' f_\tau(\alpha) + \gamma_0' f_\tau(0)(-1)^m\cos\alpha = 0, \tag{2.30}$$

in which case partial local solutions are given by

$$\tilde{\psi}_p = \frac{\gamma_0'}{2\mu} f_\tau(0)\, r^{\tau+1}\left[\sin\tau\theta\sin\theta - \frac{\sin^2\alpha}{2\sin 2\alpha}\sin(\tau \mp 1)\theta\right]. \tag{2.31}$$

Local solutions in this case do not exist.

Hydrodynamic b.c.		Thermal b.c.	
$\theta = 0$	$\theta = \alpha$	$\theta = 0$	$\theta = \alpha$
rigid	free	nf	nf
rigid	free	ft	nf
free	free	nf	nf
free	free	ft	nf

TABLE 2. Types of boundary conditions for single-phase non-isothermal flow

(3iii) When $\tau \neq 1$ and $\sin(\tau+1)\alpha = \sin(\tau-1)\alpha = 0$, local and partial local solutions exist only if $\alpha = \pi$ and if

$$\gamma_\alpha' f_\tau(\alpha) - \gamma_0' f_\tau(0)(-1)^\tau = 0. \tag{2.32}$$

Here $\tau = 2, 3, 4, \ldots$ and the streamfunction is given by

$$\psi_p = \tilde{\psi}_p = \frac{\gamma_0'}{2\mu} f_\tau(0)\, r^{\tau+1} \sin\tau\theta \sin\theta. \tag{2.33}$$

Note again that partial local solutions are not distinguished from local solutions since the normal-stress boundary condition is identically satisfied by the partial local solution form.

(4i) When $\tau = 1$ and $\sin 2\alpha \neq 0$, partial local solutions are given by

$$\tilde{\psi}_p = \frac{r^2}{4\mu}\left[\gamma_0' f_1(0)(1-\cos 2\theta) + (\gamma_\alpha' f_1(\alpha) + \gamma_0' f_1(0)\cos 2\alpha)\frac{\sin 2\theta}{\sin 2\alpha} - (\gamma_\alpha' f_1(\alpha) + \gamma_0' f_1(0))\frac{\theta}{\alpha}\right]. \tag{2.34}$$

No local solutions exist in this case.

(4ii) When $\tau = 1$ and $\sin 2\alpha = 0$, no partial local solutions exist unless

$$\gamma_\alpha' f_1(\alpha) + \gamma_0' f_1(0)\cos 2\alpha = 0 \tag{2.35}$$

in which case

$$\tilde{\psi}_p = -\frac{\gamma_0'}{4\mu} f_1(0)\, r^2\left[(\cos 2\theta - 1) + (1 - \cos 2\alpha)\frac{\theta}{\alpha}\right]. \tag{2.36}$$

When $\tau = 1$, local solutions exist when $\alpha = \pi$ and

$$\gamma_\alpha' f_1(\pi) + \gamma_0' f_1(0) = 0 \tag{2.37}$$

in which case

$$\psi_p = \frac{\gamma_0'}{2\mu} f_1(0)\, r^2 \sin^2\theta. \tag{2.38}$$

2.2.2. *Specific cases*

In this subsection we discuss four possible situations in which thermocapillary-driven flows are present for single-wedge geometries. The boundary conditions for these cases are shown in table 2. Notice that the thermal boundary condition which allows surface-tension gradients along the free surface, $\theta = \alpha$, is the no-flux condition.

Rigid/free wedge, no-flux/no-flux: In this case the thermal field is given by (2.6). We first identify the points where solvability conditions arise. First, $\tau \sin 2\alpha - \sin 2\tau\alpha = 0$

when $\alpha = \frac{1}{2}\pi$, π, or $\frac{3}{2}\pi$ so these are points with potential solvability difficulties. Next, notice that $\tau = 1$ only when $\alpha = \pi$ and $m = 1$ so the condition required for non-trivial isothermal streamfunctions with $\psi \sim r^2$ is not satisfied; i.e. $\sin 2\alpha - 2\alpha\cos 2\alpha \neq 0$, and therefore no solvability problems arise at these points.

We find that local solutions can be found only for $\alpha = \pi$. In this case the complete streamfunction, including the isothermal contribution, is given by

$$\psi = a_m r^{m+\frac{1}{2}} \sin(m-\tfrac{1}{2})\theta \sin\theta + \frac{\gamma'_\alpha}{2\mu} A_m^{th} r^{m+1} \sin m\theta \sin\theta, \tag{2.39}$$

where $m = 1, 2, 3, \ldots, a_m$ is an arbitrary constant and A_m^{th} is the arbitrary thermal coefficient of (2.6). Notice that the dominant term near $r = 0$ comes from the isothermal contribution, $\psi \sim r^{\frac{3}{2}}$. However, the constant a_m is determined by matching to an outer flow, and must be related to γ'_α. Indeed, if the flow is purely thermocapillary driven, a_m will be proportional to γ'_α.

Partial local solutions are given as follows.

For $\alpha \neq \frac{1}{2}\pi$, π, $\frac{3}{2}\pi$

$$\tilde{\psi} = -\frac{\gamma'_\alpha}{2\mu\cos\alpha} A_m^{th} r^{\tau+1} \sin\tau\theta \sin\theta + a_\sigma r^{\sigma+1} g(\theta, \alpha, \sigma), \tag{2.40}$$

where σ satisfies (2.13), and $g(\theta, \alpha, \sigma)$ is given by (2.21). Note that this streamfunction becomes ill-behaved as $\alpha \to \frac{1}{2}\pi$ or $\frac{3}{2}\pi$ unless A_m^{th} balances $\cos\alpha$ in these limits. Figure 2 shows a plot of the exponents $\tau - 1$ and $\mathrm{Re}(\sigma - 1)$ as functions of α. Near $r = 0$, the dominant term is proportional to $r^{\tau+1}$ when $\alpha < \frac{1}{2}\pi$ (thermally dominated) and $r^{\sigma+1}$ when $\alpha > \frac{1}{2}\pi$ (hydrodynamically dominated).

For $\alpha = \pi$ the streamfunction is given by

$$\begin{aligned}\tilde{\psi} = {} & a_m r^{m+\frac{1}{2}} \sin(m-\tfrac{1}{2})\theta \sin\theta + \frac{\gamma'_\alpha}{2\mu} A_m^{th} r^{m+1} \sin m\theta \sin\theta \\ & + d_m r^{m+2}[\sin(m+1)\theta\cos\theta - (m+1)\cos(m+1)\theta \sin\theta],\end{aligned} \tag{2.41}$$

where $m = 1, 2, 3, \ldots$ and the coefficients a_m and d_m are arbitrary.

For $\alpha = \frac{1}{2}\pi$, and $\frac{3}{2}\pi$ no coupled partial local solutions exist for temperature fields and streamfunctions in the class of solutions we are considering. Further discussion of this issue is given in §5.

Rigid/free wedge, fixed-temperature/no-flux: The thermal field is given by (2.7). Again, we identify points where the forcing is resonant. First, note that $\tau \sin 2\alpha - \sin 2\tau\alpha = 0$ when $\alpha = \frac{1}{2}\pi$, π, $\frac{3}{2}\pi$. Next, note that $\tau = 1$ when $\alpha = \frac{1}{2}\pi$, $\frac{3}{2}\pi$ so $\sin 2\alpha - 2\alpha\cos 2\alpha \neq 0$. Therefore no solvability problems exist when $\tau = 1$.

We find that no coupled local solutions exist but that coupled partial local solutions do exist and are given as follows.

For $\alpha \neq \frac{1}{2}\pi$, π, $\frac{3}{2}\pi$,

$$\tilde{\psi} = \frac{\gamma'_\alpha}{2\mu} \frac{B_m^{th} r^{\tau+1}}{\tau} \left[\frac{\sin\tau\theta \sin\theta}{\sin\alpha} + \frac{\tau\cos\tau\theta \sin\theta - \sin\tau\theta\cos\theta}{\cos\alpha} \right] + a_\sigma r^{\sigma+1} g(\theta, \alpha, \sigma), \tag{2.42}$$

where σ satisfies (2.13) and a_σ is an arbitrary constant. Figure 2 shows a plot of the exponents $\tau - 1$ and $\mathrm{Re}(\sigma - 1)$ as functions of α. We see that near the corner ($r \to 0$) the dominant term in the streamfunction is $r^{\tau+1}$ everywhere except for $\pi < \alpha < \frac{3}{2}\pi$, where $r^{\sigma+1}$ dominates. The stress and heat flux each are singular for $\alpha > \frac{1}{2}\pi$ with the same strength except when $\pi < \alpha < \frac{3}{2}\pi$, in which case the stress singularity is stronger.

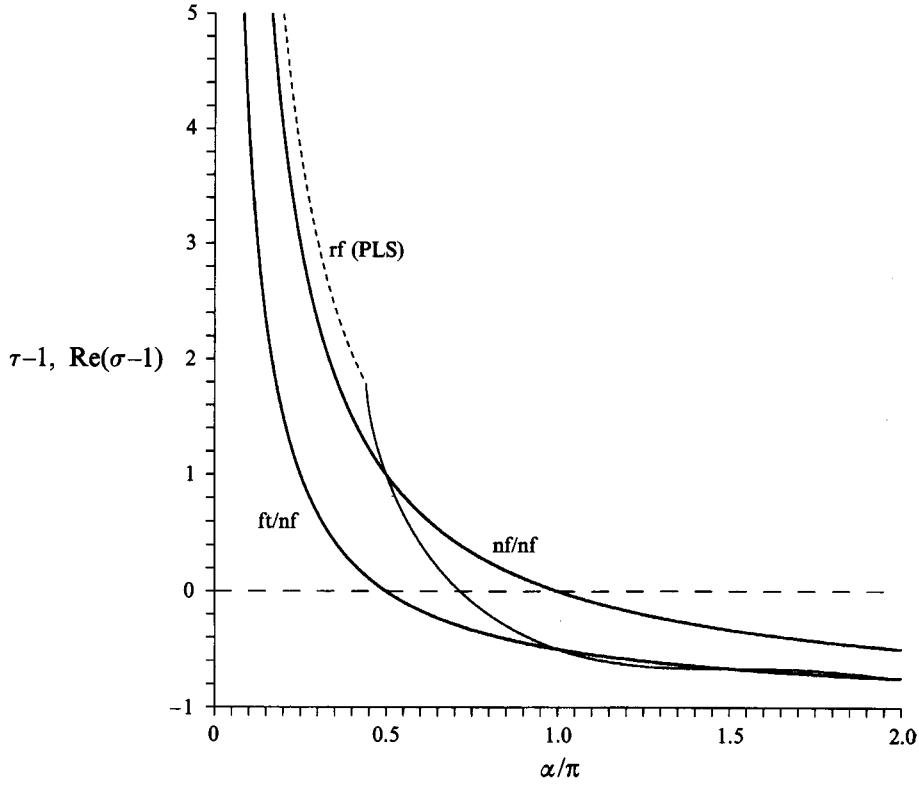

FIGURE 2. Single-phase non-isothermal flow: heat-flux and stress exponents, $\tau-1$ and $\mathrm{Re}(\sigma-1)$, respectively, for a rigid/free (rf) wedge. The stress exponent is shown for partial local solutions (PLS). The field with the smallest exponent for a given value of α is the stronger. In the ft/nf case the stress has the stronger singularity only for $\pi < \alpha < \frac{3}{2}\pi$. In the nf/nf case, the stress is the stronger field for $\alpha > \frac{1}{2}\pi$ while the heat flux is stronger for $\alpha < \frac{1}{2}\pi$. The dashed portion of the stress exponent indicates that its imaginary part is non-zero.

For $\alpha = \frac{1}{2}\pi$ we have $\tau = 2m+1 = 1, 3, 5, \ldots$. Here only the first mode, $\tau = 1$, is allowed by the solvability condition. Therefore, the thermal field is given by

$$T = T_W + B_0^{th} r \sin\theta \tag{2.43}$$

and the resulting streamfunction is given by

$$\tilde{\psi} = -\frac{\gamma'_\alpha}{4\mu} B_0^{th} r^2 \left[-1 + \frac{4}{\pi}\theta + \cos 2\theta - \frac{2}{\pi}\sin 2\theta \right] + a_m r^{2m+3} \sin 2(m+1)\theta \sin\theta$$
$$+ d_m r^{2m+4} [\sin(2m+3)\theta \cos\theta - (2m+3)\cos(2m+3)\theta \sin\theta], \tag{2.44}$$

where $m = 0, 1, 2, \ldots$, and the coefficients B_0^{th}, a_m, and d_m are arbitrary. Notice here that the dominant term near $r = 0$ is the term proportional to r^2. The heat flux is regular but, owing to the term proportional to $r^2\theta$, the stress field has a logarithmic singularity.

For $\alpha = \frac{3}{2}\pi$ we have $\tau = \frac{2}{3}m + \frac{1}{3} = \frac{1}{3}, 1, \frac{5}{3}, \ldots$. Here we find similar results to the case $\alpha = \frac{1}{2}\pi$. The thermal field is given by

$$T = T_W + B_1^{th} r \sin\theta \tag{2.45}$$

and the resulting streamfunction is given by

$$\tilde{\psi} = -\frac{\gamma'_\alpha}{4\mu} B_1^{th} r^2 \left[1 - \frac{4}{3\pi}\theta - \cos 2\theta + \frac{2}{3\pi}\sin 2\theta\right] + d_\sigma r^{\sigma+1}[\sin\sigma\theta\cos\theta - \sigma\cos\sigma\theta\sin\theta] + a_\sigma r^{\sigma+1}\sin\sigma\theta\sin\theta, \quad (2.46)$$

where $\sigma = \frac{1}{3}, \frac{5}{3}, \frac{7}{3}, \ldots$ for the d_σ terms and $\sigma = \frac{2}{3}, \frac{4}{3}, 2, \ldots$ for the a_σ terms. Again B_1^{th}, d_σ, and a_σ are arbitrary constants. Here the heat flux is regular but the stress is singular ($\sim r^{-\frac{1}{3}}$). Notice that although there is again a logarithmic singularity at $r = 0$ arising from the term $r^2\theta$, it is not the dominant singularity.

For $\alpha = \pi$ no coupled partial local solutions or local solutions exist. For further discussion of this see §5.

Free/free wedge, no-flux/no-flux: In this case the thermal field is given by (2.6). Here, $\sin(\tau+1)\alpha \sin(\tau-1)\alpha = 0$ only when $\alpha = \pi$.

We find that local solutions exist only when $\alpha = \pi$ and only for the case where $\gamma'_0 = \gamma'_\alpha$. Here the streamfunction is given by

$$\psi = B_0 r\sin\theta + \frac{\gamma'_0}{2\mu} A_m^{th} r^{m+1}\sin m\theta\sin\theta + b_m r^{m+2}\cos(m+1)\theta\sin\theta, \quad (2.47)$$

where $m = 1, 2, 3, \ldots$ and the coefficients B_0, A_m^{th}, and b_m are arbitrary.

Next, for partial local solutions we find that for $\alpha \neq \pi$ the streamfunction is given by

$$\tilde{\psi} = \tilde{\psi}_I + \frac{1}{2\mu} A_m^{th} r^{\tau+1}\left[\gamma'_0\sin\tau\theta\sin\theta + \frac{\gamma'_\alpha + \gamma'_0\cos\alpha}{\sin\alpha}\sin\tau\theta\cos\theta\right], \quad (2.48)$$

where $\tilde{\psi}_I$ represents the isothermal contribution proportional to $r^{\sigma+1}$ and is given as a function of α by Anderson & Davis (1993, equations (2.35), (2.36), or (2.38)).

Figure 3 shows the heat-flux and stress-field exponents, $\tau - 1$ and $\sigma - 1$, respectively, as functions of α (note that σ is real-valued in this case). The dominant term in the stream-function comes from $r^{\sigma+1}$ for all values of α. Consequently, the stress is always more singular than the heat flux.

For $\alpha = \pi$ we have $\tau = 1, 2, 3, \ldots$ and coupled solutions exist only in the case where $\gamma'_0 = \gamma'_\alpha$. Here the streamfunction is given by

$$\tilde{\psi} = \tilde{B}_0 r\sin\theta + \tilde{B}_1 r^2\sin 2\theta + \frac{\gamma'_0}{2\mu} A_m^{th} r^{m+1}\sin m\theta\sin\theta + r^{m+2}[b_m\sin(m+2)\theta + d_m\sin m\theta], \quad (2.49)$$

where $m = 1, 2, 3, \ldots$. For this solution both the heat flux and stress are regular.

Free/free wedge, fixed-temperature/no-flux: Here the thermocapillary effect will be present only on $\theta = \alpha$, since $f_\tau(0) = 0$. The thermal field is given by (2.7). Here, $\sin(\tau+1)\alpha\sin(\tau-1)\alpha = 0$ when $\alpha = \frac{1}{2}\pi$ or $\frac{3}{2}\pi$ so these are the points where solvability conditions arise.

We find that local solutions exist only for $\alpha = \pi$ and are given by

$$\psi = -\frac{\gamma'_\alpha}{2\mu} B_m^{th} r^{m+\frac{3}{2}}\cos(m+\tfrac{1}{2})\theta\sin\theta + B_0 r\sin\theta + b_m r^{m+3}\cos(m+2)\theta\sin\theta, \quad (2.50)$$

where $m = 0, 1, 2, \ldots$. Here, the heat flux and stress have square-root singularities.

Partial local solutions are given as follows.

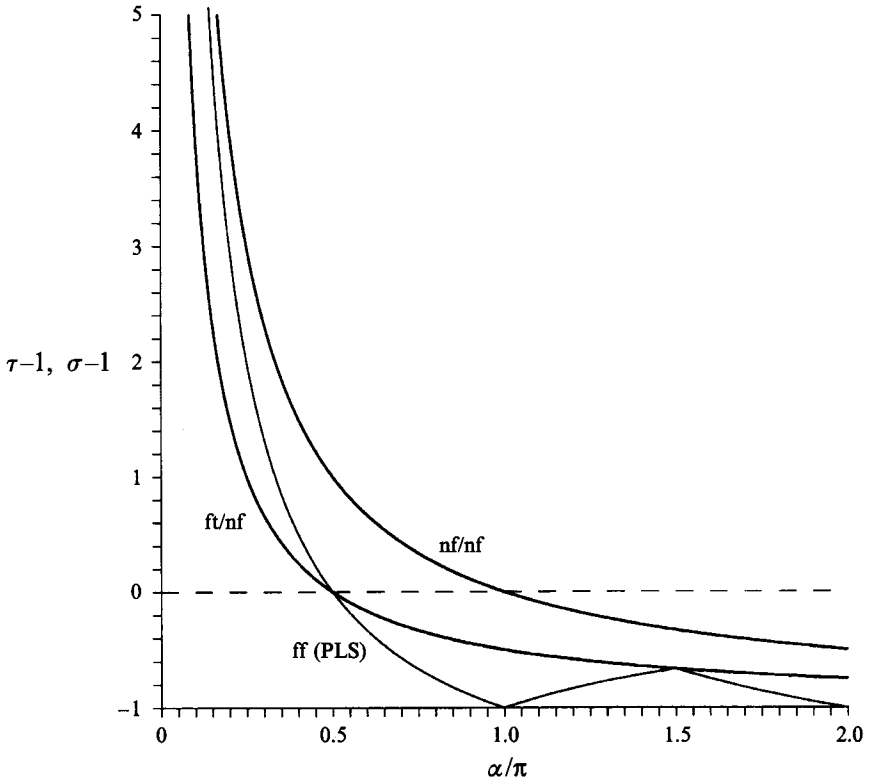

FIGURE 3. Single-phase non-isothermal flow: heat-flux and stress exponents, $\tau-1$ and $\sigma-1$, respectively, for a free/free (ff) wedge. The stress exponent shown is for partial local solutions. In the ft/nf case, the stress is the stronger singularity for $\alpha > \frac{1}{2}\pi$. The heat flux is the stronger field for $\alpha < \frac{1}{2}\pi$ but neither field is singular. In the nf/nf case, the stress is always the stronger field. Note that both τ and σ are real.

For $\alpha \neq \frac{1}{2}\pi, \frac{3}{2}\pi$

$$\tilde{\psi} = \tilde{\psi}_I + \frac{\gamma'_\alpha B_m^{th}}{2\mu \cos\alpha} r^{\tau+1} \cos\tau\theta \sin\theta, \tag{2.51}$$

where $\tilde{\psi}_I$ refers to the isothermal contribution proportional to $r^{\sigma+1}$ and is given in Anderson & Davis (1993, equations (2.35) or (2.37)), depending on α.

Figure 3 shows the exponents, $\tau-1$ and $\sigma-1$ for this case. The dominant term in the streamfunction corresponds to $r^{\tau+1}$ when $\alpha < \frac{1}{2}\pi$ and to $r^{\sigma+1}$ when $\alpha > \frac{1}{2}\pi$. The heat flux and stress are singular for $\alpha > \frac{1}{2}\pi$ with the stress having the stronger singularity.

If $\alpha = \frac{1}{2}\pi$, 2π no coupled solutions exist. Again, see §5.

Finally, for the rigid/rigid case or the rigid/free, free/free cases where $\gamma' = 0$ there is no local coupling between the thermal and flow fields. Consequently, the solutions to the 'non-isothermal' flow problem are just those for the single fields. That is, $\psi \sim r^{\sigma+1}$ and $T \sim r^{\tau}$. Figures 2–4 show the heat-flux and stress exponents for rigid/free wedge, free/free wedge, and the rigid/rigid wedge, respectively. Note particularly that when the stress exponent has a non-zero imaginary part (dashed portions of the curves in figures 2 and 4), Moffatt vortices are present. However, the heat-flux exponent is real; hence, the thermal field is monotonic in r. Therefore, locally, there is a coexistence of a flow with Moffatt vortices and a monotonic thermal field. This type of solution is possible because, locally, there is no advection in the energy equation. The singular

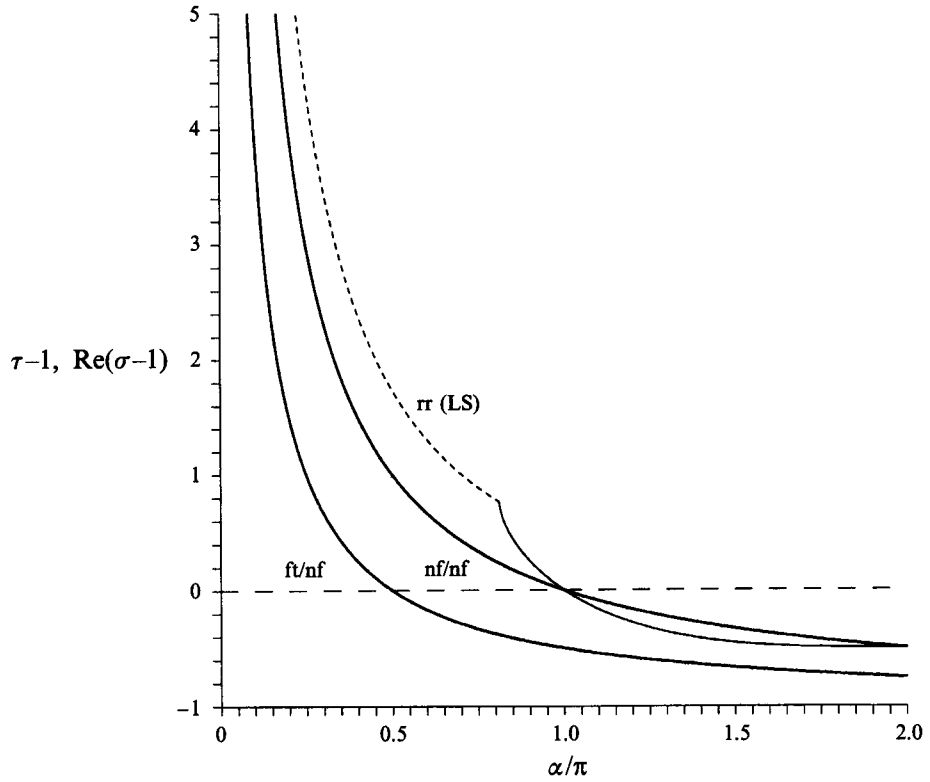

FIGURE 4. Single-phase non-isothermal flow: heat-flux and stress exponents, $\tau-1$ and $\mathrm{Re}(\sigma-1)$, respectively, for a rigid/rigid (rr) wedge. In the ft/nf case, the heat flux is the stronger singularity for $\alpha > \frac{1}{2}\pi$. In the nf/nf case, both stress and heat flux become singular for $\alpha > \pi$ but the stress is the stronger singularity. The dashed portion of the stress exponent indicates that its imaginary part is non-zero.

nature of the heat flux and stress can be identified for the rigid/free wedge and the free/free wedge in figures 2 and 3. For the rigid/rigid wedge (figure 4) the no-flux/no-flux case has singular heat flux and stress for $\alpha > \pi$ with the stress being the stronger singularity. For the fixed-temperature/no-flux case the heat is singular for $\alpha > \frac{1}{2}\pi$.

3. Two-phase systems

We now consider two-phase problems with a double-wedge geometry. Here the outer boundaries are given by $\theta = -\alpha_1$ and $\theta = \alpha_2$ and the interface separating the two phases 1 and 2 is given by $\theta = 0$; the total wedge angle is $\alpha \equiv \alpha_1 + \alpha_2$. We shall first consider pure heat transfer in two phases, and then two-phase non-isothermal flow for a solid/liquid wedge.

3.1. *Thermal fields*

In this section we consider heat transfer only. We take the thermal conductivity in regions 1 and 2 to be k_1 and k_2, respectively and solve for the temperatures T_1 and T_2 which locally satisfy Laplace's equations. The thermal boundary conditions on the outer boundaries will be the same as in the single-phase cases. Along the dividing boundary, $\theta = 0$, we require continuous temperatures and heat fluxes. The boundary conditions for the three cases we shall consider are summarized in table 3. Here

	$\theta = -\alpha_1$	$\theta = 0$	$\theta = \alpha_2$
Case 1	nf	continuity	nf
Case 2	ft	continuity	nf
Case 3	ft	continuity	ft

TABLE 3. Types of thermodynamic boundary conditions for a double wedge

'continuity' corresponds to the conditions of continuous temperatures and heat fluxes across the interface $\theta = 0$ as given by

$$[T_i]_{i-1}^{i-2} = \left[k_i \frac{\partial T_i}{\partial \theta}\right]_{i-1}^{i-2} = 0, \tag{3.1}$$

and 'nf' and 'ft' refer to no-flux and fixed-temperature conditions, respectively, as described in §2.1. Keller (1987) has analysed the subcase, $\alpha = \frac{1}{2}\pi$, of Case 2 in which the harmonic function was related to the conductance of a material arranged in an array of blocks with alternating high/low conductivity.

The solutions in these cases are as follows.

For Case 1

$$T_1 = D_1^{th} + A^{th} r^\tau \cos\tau(\theta+\alpha_1), \tag{3.2a}$$

$$T_2 = D_1^{th} + \frac{A^{th}}{k} r^\tau [\cos\tau(\theta+\alpha_1) + (k-1)\cos\tau\alpha_1 \cos\tau\theta], \tag{3.2b}$$

where

$$\sin\tau\alpha = (1-k)\cos\tau\alpha_1 \sin\tau\alpha_2. \tag{3.3}$$

For Case 2

$$T_1 = T_{\alpha_1} + A^{th} r^\tau [\cos\tau(\theta-\alpha_2) + (k-1)\sin\tau\alpha_2 \sin\tau\theta], \tag{3.4a}$$

$$T_2 = T_{\alpha_1} + A^{th} r^\tau \cos\tau(\theta-\alpha_2), \tag{3.4b}$$

where

$$\cos\tau\alpha = (k-1)\sin\tau\alpha_2 \sin\tau\alpha_1. \tag{3.5}$$

For Case 3

$$T_1 = T_{\alpha_1} + k\frac{T_{\alpha_2} - T_{\alpha_1}}{\alpha_2 + k\alpha_1}(\theta+\alpha_1) + A^{th} r^\tau \sin\tau(\theta+\alpha_1), \tag{3.6a}$$

$$T_2 = T_{\alpha_1} + \frac{T_{\alpha_2} - T_{\alpha_1}}{\alpha_2 + k\alpha_1}(\theta+k\alpha_1) + \frac{A^{th}}{k} r^\tau [\sin\tau(\theta+\alpha_1) + (k-1)\sin\tau\alpha_1 \cos\tau\theta], \tag{3.6b}$$

where

$$\sin\tau\alpha = (1-k)\sin\tau\alpha_1 \cos\tau\alpha_2. \tag{3.7}$$

Here, T_{α_1} and T_{α_2} correspond to the fixed temperature values on $\theta = -\alpha_1$ and α_2 respectively, and $k \equiv k_2/k_1$ is the conductivity ratio. Note that if the boundary conditions in Case 2 were reversed (i.e. no flux on $\theta = -\alpha_1$ and fixed temperature on $\theta = \alpha_2$), the resulting thermal field, with T_1 and T_2 interchanged, could be found by replacing (k, α_2, α_1) by $(1/k, -\alpha_1, -\alpha_2)$ in (3.4) and (3.5).

Conditions (3.3), (3.5), and (3.7) determine τ for a given geometry and conductivity ratio, k. These conditions have symmetry characteristics that simplify the analysis. First note that, in all three cases, if $k = 1$, then we can recover the single-phase results of §2.1 by letting $\theta \to \theta - \alpha_1$ and interpreting α as the single-phase angle. When $k = 1$, the two phases are thermodynamically indistinguishable and hence are seen as a single phase. In Case 1, given that $(k, \tau, \alpha_2, \alpha_1)$ satisfies condition (3.3), then $(1/k, \tau, \alpha_1, \alpha_2)$ also

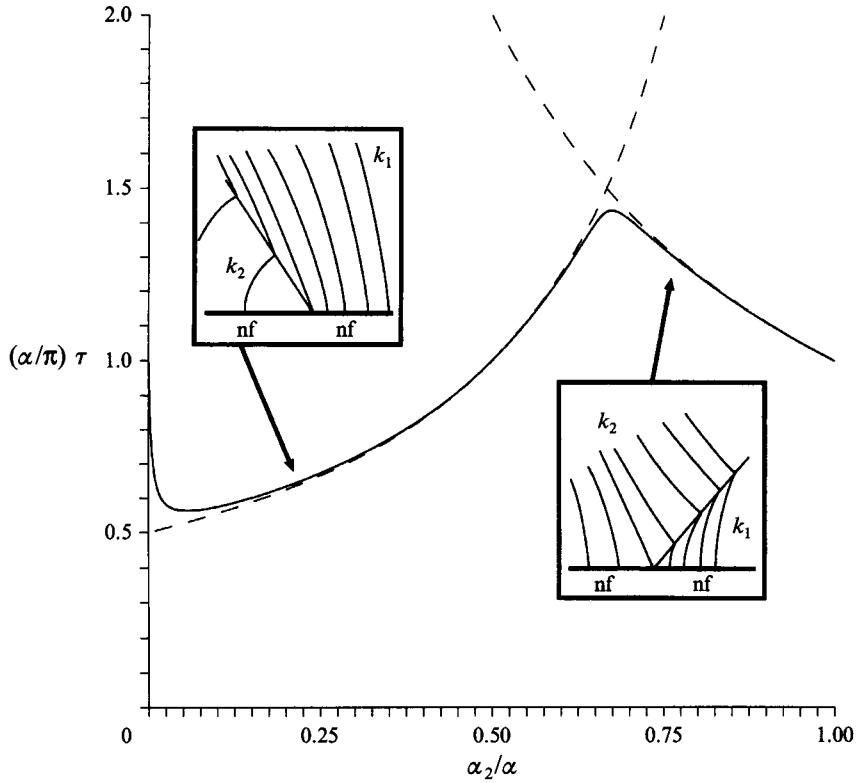

FIGURE 5. Two-phase pure heat transfer: the thermal field exponent as a function of the wedge angles for conductivity ratios $k = 100$ (solid curve) and $k = \infty$ (dashed curves) for Case 1. As $k \to \infty$ the roots approach solutions of $\cos\tau\alpha_1 \sin\tau\alpha_2 = 0$. Note that only the dashed curve on the right is obtained from the single-phase analysis when phase 1 is completely neglected. The sketched insets show the two types of modes which are present in the two-phase analysis in the limit $k \to \infty$. The inset on the left shows the heat-flux mode in which the phase with the larger conductivity is at a relatively constant temperature. The inset on the right shows the temperature mode in which the temperature in both phases is substantial along $\theta = 0$. In each case the temperature gradient at $\theta = 0$ in phase 1 is much larger than that in phase 2; however, the heat fluxes balance owing to the large conductivity ratio.

satisfies the condition. Therefore, we can limit our analysis to $k > 1$. In Case 2, given that $(k, \tau, \alpha_2, \alpha_1)$ satisfies condition (3.5), then $(k, \tau, \alpha_1, \alpha_2)$ also satisfies the condition. In Case 3, there is the same type of symmetry as in Case 1. In fact, given a solution $(k, \tau, \alpha_1, \alpha_2)$ satisfying condition (3.3), then $(k, \tau, \alpha_2, \alpha_1)$ satisfies condition (3.7). Therefore the roots, τ, for Case 3 can be deduced directly from those of Case 1.

We have analysed these nonlinear conditions numerically as well as asymptotically to find the roots, τ, as functions of α_2 for given values of k and α. Scaled versions of the numerically computed roots are shown in figures 5–7. These figures show $(\alpha/\pi)\tau$ *vs.* α_2/α for various values of k. Note that just as in the single-phase case, τ is always real-valued. From these plots we see a strong dependence on the conductivity ratio, k.

Figure 5 (Case 1), shows the smallest root for $k = 100.0$. We see that as $k \to \infty$ the roots of (3.3) approach values satisfying $\cos\tau\alpha_1 \sin\tau\alpha_2 = 0$. Physically, $k = \infty$ represents heat transfer in a single wedge between two no-flux boundaries. Therefore we expect to find roots, τ, which satisfy $\sin\tau\alpha_2 = 0$ as in the single-phase problem. However, the two-phase problem has additional roots from the phase with

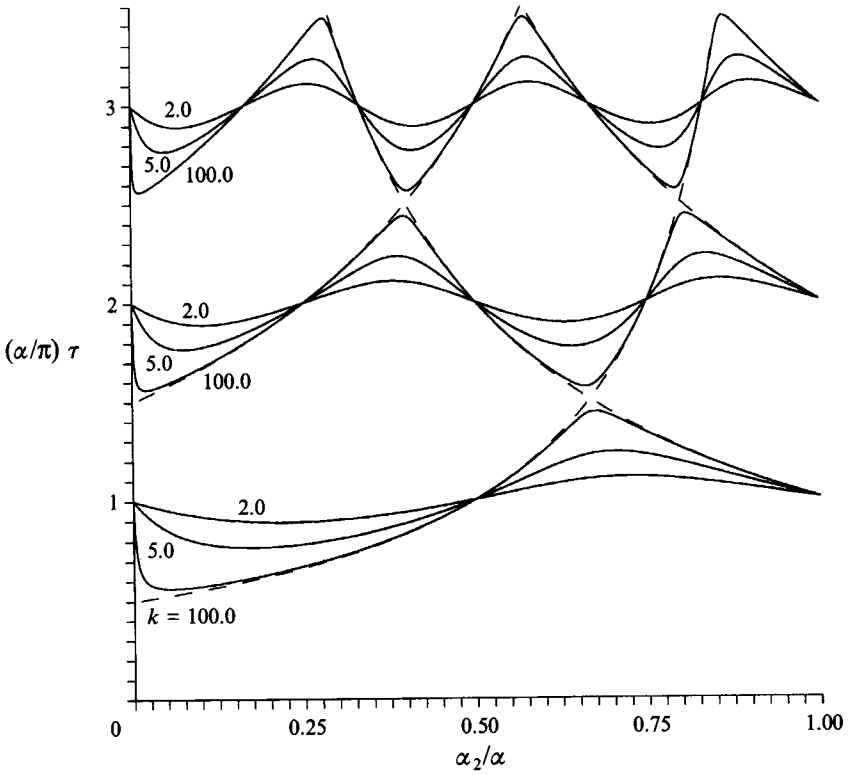

FIGURE 6. Two-phase pure heat transfer: the first three scaled thermal field exponents as functions of the wedge angles for various conductivity ratios k for Case 1. As $k \to \infty$ the roots approach solutions of $\cos \tau\alpha_1 \sin \tau\alpha_2 = 0$ and show boundary-layer behaviour. The dashed curves show the solution for $k = \infty$. Note the addition of a second mode not obtained in the single-phase analysis. For $k = 1$ the value of τ is independent of the individual wedge angles and depends only on the total wedge angle α.

asymptotically small conductivity satisfying $\cos \tau\alpha_1 = 0$. Hence, the results for $k = \infty$ in the two-phase problem have two roots, shown as the dashed curves in figure 5. Figure 6 shows higher modes as well and we see that the dashed roots form a grid-like pattern. The smallest value of $\tau - 1$ for $0 < \alpha_2 < \alpha$ is a combination of the two separate branches that intersect.

Proudman & Asadullah (1988) identified the same type of behaviour for two-fluid corner flow with total wedge angle π. They identified two modes of flow in the limit of vanishing viscosity ratio between the two fluids: a 'velocity' mode in which the velocities on the separating interface were $O(1)$, and a 'stress' mode in which the more-viscous fluid was relatively static but the stresses were equal in magnitude.

In direct analogy to their work, we term the two modes of heat flow found here for $k \to \infty$ the 'temperature' mode and the 'heat flux' mode. First, the temperature mode corresponds to an $O(1)$ temperature on the interface $\theta = 0$. This mode is shown in the lower right inset in figure 5. The temperature gradient normal to the interface $\theta = 0$ is nearly zero in phase 2, while it is substantial in phase 1; the heat fluxes still balance as a result of k being large. This is analogous to the velocity mode in Proudman & Asadullah (1988). Second, the heat flux mode corresponds to nearly zero temperature in both phases at $\theta = 0$ (neglecting any additive constant temperature). This mode is shown in the upper left inset in figure 5. There again is a nearly zero temperature

gradient normal to the interface in phase 2 at $\theta = 0$ and a substantial gradient normal to the interface $\theta = 0$ in phase 1, but again, owing to the disparate conductivities, the heat fluxes balance. In this mode the temperature is relatively constant in phase 2, the phase with the larger conductivity. The temperature field in phase 1 looks like that in a single wedge with a no-flux condition on $\theta = -\alpha_1$ and a fixed-temperature condition on $\theta = 0$. This is exactly analogous to the stress mode identified by Proudman & Asadullah (1988).

An important feature here is the comparison of the exponent τ for the single-phase case and the two-phase case in the limit of large or small conductivity ratio. In the single-phase case we find that $\tau \to \infty$ as $\alpha_2 \to 0$ but when two phases are considered, τ remains finite as $\alpha_2 \to 0$ and $\alpha_1 \neq 0$. This shows that the limit $k \to \infty$ (or $k \to 0$) is singular and the consideration of a second phase may be important even for extreme values of k.

The intersections of the branches for $k = \infty$ imply the existence of double roots, which are important for understanding the behaviour of the roots when $k \neq \infty$. Since τ is real-valued the roots for $k = \infty$ always intersect. When k is perturbed from infinity, a root splitting occurs; two non-intersecting branches are formed, an upper and a lower. Notice that the lowest branch in figure 6 for large k is involved in one such splitting, the second branch has three such points, and the third has five. This behaviour is analogous to the root splitting described by Anderson & Davis (1993) for two-fluid flow for the same geometry. In their analysis, the root σ was in general complex and therefore with vanishing viscosity ratio, $\mu = 0$ (analogous to $k = \infty$ here), the roots did not necessarily intersect in the complex plane; hence, the range in which there were double roots was limited.

To describe analytically this splitting for the lowest root for $k \to \infty$ for Case 1 we match the two outer solution branches corresponding to the solutions for $k = \infty$ with an inner solution valid near the intersection of these two solutions. A boundary-layer correction is included which takes into account the non-uniformity present when $\alpha_2 \to 0$ and $k \to \infty$. The uniformly valid expression for the smallest value of τ is given by

$$\tau \sim \tau_0 + (\tfrac{3}{2})^3 \frac{\pi}{\alpha^2} |\alpha_2 - \tfrac{2}{3}\alpha| - k^{-\frac{1}{2}} \frac{3}{2\alpha} \left[2 + (\tfrac{3}{2})^4 \left(\frac{\pi}{\alpha} \right)^2 (\alpha_2 - \tfrac{2}{3}\alpha)^2 k \right]^{\frac{1}{2}} + Z(\eta) - \frac{\pi}{2\alpha} + \ldots, \quad (3.8)$$

where

$$\tau_0 = \begin{cases} \pi/(2(\alpha - \alpha_2)) & \text{for} \quad \alpha_2 \leqslant \tfrac{2}{3}\alpha \\ \pi/\alpha_2 & \text{for} \quad \alpha_2 > \tfrac{2}{3}\alpha, \end{cases} \quad (3.9)$$

$\eta \equiv \alpha_2 k$, and $Z(\eta)$ satisfies $\eta Z(\eta) + \tan Z(\eta)\,\alpha = 0$. Since $Z(\eta)$ must still be calculated numerically, this expression is most useful outside an $O(1/k)$ neighbourhood near $\alpha_2 = 0$ where one can ignore the last two terms, which represent the corrected solution near the boundary layer at $\alpha_2 = 0$.

For Case 2, a similar root splitting occurs for $k \to 0$ and $k \to \infty$. Figure 7 shows the smallest of these roots for various k. In the limit as $k \to 0$ the roots of (3.5) satisfy $\cos \tau\alpha_1 \cos \tau\alpha_2 = 0$. Here we expect that τ satisfies $\cos \tau\alpha_1 = 0$ as in the single-phase problem for a wedge with fixed temperature on $\theta = -\alpha_1$ and no flux on $\theta = 0$ but we pick up additional roots satisfying $\cos \tau\alpha_2 = 0$ from the second phase.

Again we identify the temperature and heat-flux modes. These two modes have the same properties as those shown for Case 1 in figure 5. The temperature mode corresponds to the left half of the curves shown for $k \to 0$ (i.e. $\alpha_2 < \alpha_1$) and the heat-flux mode corresponds to the right half (see figure 7). In the temperature mode, the thermal field in phase 1, the phase with larger conductivity, is that predicted by the single-phase analysis. The heat-flux mode is the 'new' mode and corresponds to a

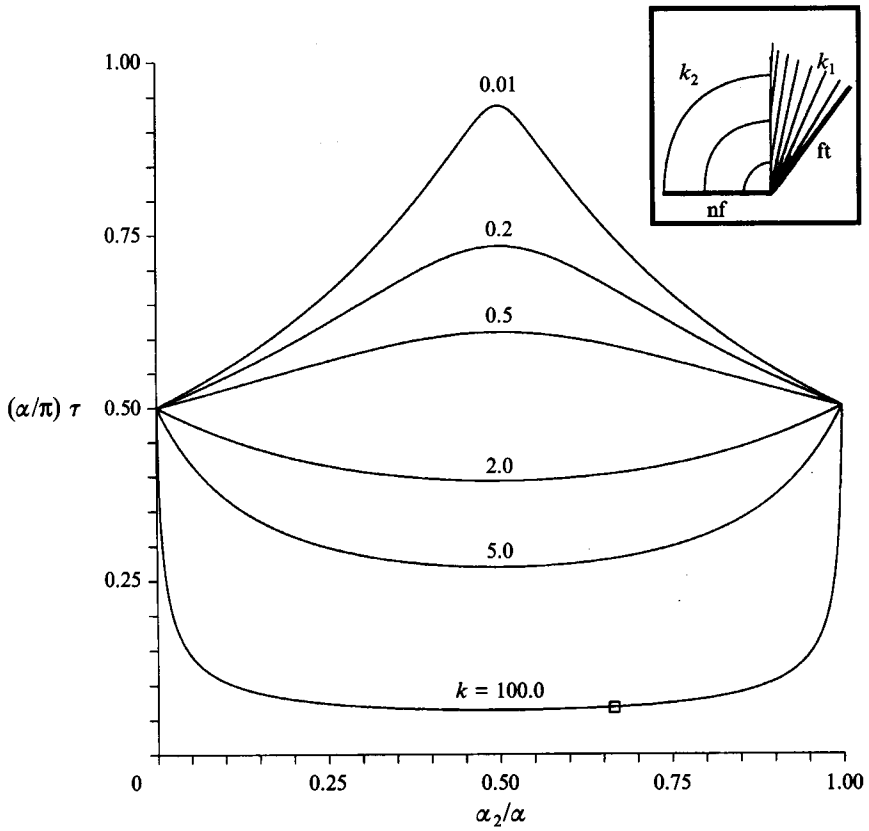

FIGURE 7. Two-phase pure heat transfer: the smallest scaled thermal field exponent as a function of the wedge angles for various conductivity ratios, k, for Case 2. As $k \to \infty$ this root approaches zero non-uniformly. As $k \to 0$ this root approaches solutions of $\cos\tau\alpha_1 \cos\tau\alpha_2 = 0$ corresponding to two different modes. For $k = 1$ the value of τ is independent of the individual wedge angles and depends only on the total wedge angle α. The inset shows isotherms corresponding to the point marked on the curve for $k = 100.0$. Here, the temperature in phase 1 is approximately linear in θ while that in phase 2 is logarithmic in r.

nearly constant temperature in phase 1 and a temperature distribution in phase 2 corresponding to a fixed-temperature condition on $\theta = 0$ and no-flux condition on $\theta = \alpha_2$.

We again use singular perturbation methods to obtain an analytical solution for τ for $k \ll 1$. Here we find that the uniformly valid expression for the smallest value of τ is given by

$$\tau \sim \frac{\pi}{\alpha + 2|\alpha_2 - \frac{1}{2}\alpha|} + \frac{2\pi}{\alpha^2}|\alpha_2 - \tfrac{1}{2}\alpha| - k^{\frac{1}{2}}\frac{2}{\alpha}\left[1 + \left(\frac{\pi}{\alpha}\right)^2 (\alpha_2 - \tfrac{1}{2}\alpha)^2 \frac{1}{k}\right]^{\frac{1}{2}} + \ldots. \tag{3.10}$$

In the limit $k \to \infty$ for Case 2 there is a root-splitting behaviour for the higher modes similar to that for $k \to 0$. However, the smallest value of τ approaches zero non-uniformly as $k \to \infty$ (see figure 7). We again use singular perturbation methods to express the solution for the lowest mode analytically and find that

$$\tau \sim \frac{k^{-\frac{1}{2}}}{(\alpha_2 \alpha_1)^{\frac{1}{2}}} + \left[A(\eta_2) + A(\eta_1) - \frac{k^{-\frac{1}{2}}}{(\alpha_2 \alpha)^{\frac{1}{2}}} - \frac{k^{-\frac{1}{2}}}{(\alpha_1 \alpha)^{\frac{1}{2}}}\right] + \ldots, \tag{3.11}$$

where $A(\eta)$ satisfies $A(\eta)\,\eta\tan A(\eta)\,\alpha = 1$ and $\eta_2 \equiv \alpha_2 k$ and $\eta_1 \equiv \alpha_1 k$. This expression will be most useful away from the two boundary layers near $\alpha_2 = 0$, and α where the bracketed terms can be neglected. These boundary layers each have thickness $O(1/k)$.

This limit leads to a different type of temperature distribution. We find that as $k \to \infty$ the temperature in phase 2 goes like $\ln r$, independent of θ, while the distribution in phase 1 is approximately linear in θ, independent of r. An example of this mode is shown in the inset in figure 7. We shall discuss this solution further in §5.

For k near unity, the roots approach constant values (for fixed α) in all cases. For this limit we have found expressions for τ using a regular perturbation expansion in powers of $k-1$. We find

$$\tau = \tau_0 - (k-1)\frac{\sin 2\tau_0\alpha_2}{2\alpha} + (k-1)^2\left[\frac{\sin 2\tau_0\alpha_2}{2\alpha^2}[\alpha\sin^2\tau_0\alpha_2 + \alpha_2\cos 2\tau_0\alpha_2]\right] + O((k-1)^3), \quad (3.12)$$

where $\tau_0 = m\pi/\alpha$ for $m = 1, 2, 3, \ldots$ in Case 1 and $\tau_0 = (l+\frac{1}{2})\pi/\alpha$ for $l = 0, 1, 2, \ldots$ in Case 2.

The above asymptotic expressions for $k \to 0, 1, \infty$ agree well with the numerically computed values.

In contrast to the single-phase pure-heat-transfer results, the value of τ now has additional parametric dependence through the geometry and the conductivity ratio. A complete description of the regions in parameter space separating singular heat flux from non-singular heat flux is shown in figures 8 and 9 for Cases 1 and 2, respectively. The shaded regions correspond to singular heat fluxes (i.e. $\tau - 1 < 0$) while the unshaded regions correspond to non-singular heat fluxes (i.e. $\tau - 1 > 0$). The boundary between the shaded and unshaded regions corresponds to $\tau - 1 = 0$. In figure 8 this boundary is given by

$$k = \frac{\tan(\alpha_2 - \alpha)}{\tan\alpha_2} \quad (3.13)$$

from which we can deduce that the critical values of α_2 and k are given by

$$\alpha_2^c = \tfrac{1}{2}\alpha \pm \tfrac{1}{4}\pi, \quad (3.14a)$$

$$k_c^+ = \tan^2(\tfrac{1}{4}\pi - \tfrac{1}{2}\alpha), \quad (3.14b)$$

$$k_c^- = 1/k_c^+. \quad (3.14c)$$

In figure 9 this boundary is given by

$$k = \frac{1}{\tan\alpha_2\tan(\alpha - \alpha_2)} \quad (3.15)$$

from which we can deduce that the critical values of α_2 and k are given by

$$\alpha_2^c = \tfrac{1}{2}\alpha, \quad (3.16a)$$

$$k_c = 1/\tan^2\alpha_2^c. \quad (3.16b)$$

In Case 1, no singularities are present when $\alpha \leqslant \frac{1}{2}\pi$ and singularities are always present when $\alpha \geqslant \frac{3}{2}\pi$. In Case 2 singularities are always present when $\alpha \geqslant \pi$. As in the single-phase case, as α decreases the heat flux becomes less singular (or not singular at all) and as α increases the reverse is true. In Case 1, for $\alpha_2 < \alpha_1$ as k increases τ decreases and for $\alpha_2 > \alpha_1$ the opposite is true. This shows that when the smaller of the two wedges has the larger conductivity the singularity is stronger than when the smaller of the two wedges has the smaller conductivity. For Case 2 the singularity is stronger when the

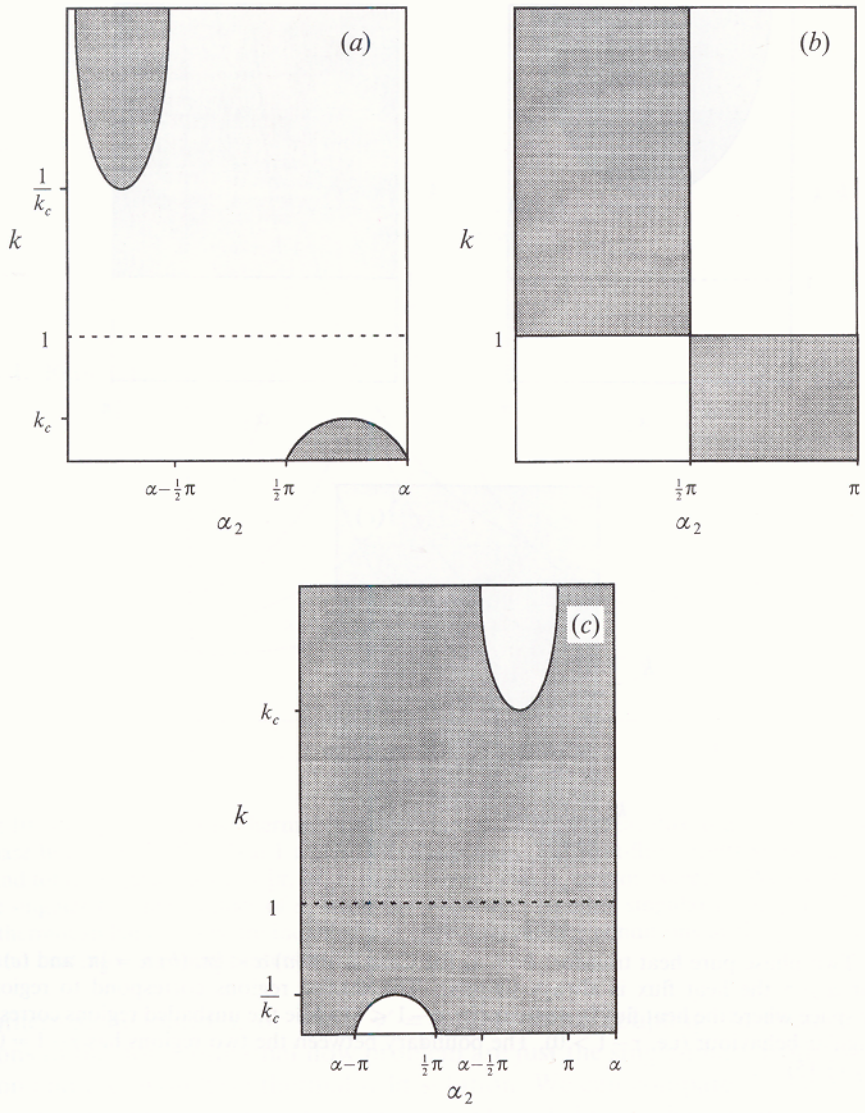

FIGURE 8. Two-phase pure heat transfer: k *vs.* α_2 for Case 1 for (*a*) $\frac{1}{2}\pi < \alpha < \pi$, (*b*) $\alpha = \pi$, and (*c*) $\pi < \alpha < \frac{3}{2}\pi$. For $\alpha \leqslant \frac{1}{2}\pi$ the heat flux is never singular while for $\alpha \geqslant \frac{3}{2}\pi$ the heat flux is always singular. The shaded regions correspond to regions in parameter space where the heat flux is singular (i.e. $\tau - 1 < 1$) while the unshaded regions correspond to non-singular behaviour (i.e. $\tau - 1 > 0$). The boundary between the two regions has $\tau - 1 = 0$ and is given by (3.13).

conductivity in the wedge with the fixed-temperature boundary condition is smaller (i.e. $k > 1$). This holds regardless of the size of either of the two individual wedges.

Observations analogous to those made for the single-phase thermal-field results found in §2.1 can be made here. First, τ is always real-valued. Secondly, the same hierarchy in terms of heat-flux singularity, which was present in the single-phase thermal-field analysis, is present here. The no-flux/continuity/no-flux case (Case 1) shows the least singular behaviour, the fixed-temperature/continuity/no-flux case (Case 2) is the next most singular, and the fixed-temperature/continuity/fixed-temperature case (Case 3) is the most singular. Note that although the value of τ in Case 3 is related to that in Case 1, as in the single-phase analysis, the heat flux in Case

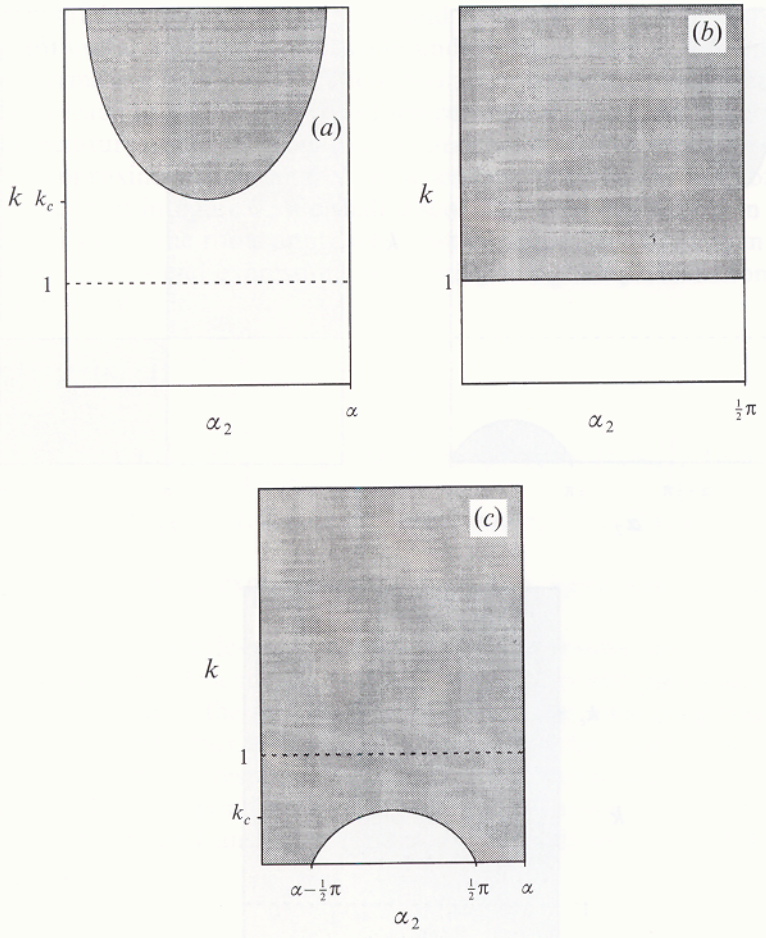

FIGURE 9. Two-phase pure heat transfer: k *vs.* a_2 for Case 2 for (*a*) $\alpha < \frac{1}{2}\pi$, (*b*) $\alpha = \frac{1}{2}\pi$, and (*c*) $\frac{1}{2}\pi < \alpha < \pi$. For $\alpha \geqslant \pi$ the heat flux is always singular. The shaded regions correspond to regions in parameter space where the heat flux is singular (i.e. $\tau - 1 < 1$) while the unshaded regions correspond to non-singular behaviour (i.e. $\tau - 1 > 0$). The boundary between the two regions has $\tau - 1 = 0$ and is given by (3.15).

3 exhibits a r^{-1} behaviour due to the term linear in θ in the expressions for the temperature fields. We also note that the ratio between the two individual wedge angles, rather than the actual values of these angles, is the important parameter in determining the 'shape' of these curves. However, the actual value of α determines the vertical scaling of τ and the subsequent spacing between the higher roots. That is, as α increases, the value of τ decreases and the roots tends to compress; and as α decreases, the value of τ increases and the roots tend to spread out. Note that in figure 6 the roots for $1/k$ can be found simply by reflecting the roots for k about $\alpha_2 = \frac{1}{2}\alpha$. In figure 7 the roots are symmetric about $\alpha_2 = \frac{1}{2}\alpha$. We find that the presence of a second phase leads to a second mode of heat flow not obtained from the single-phase analysis.

3.2. *Non-isothermal flow*

In an analogous fashion to non-isothermal single-phase flow we consider non-isothermal two-phase flow in a solid/liquid wedge. Here there is fluid flow in a single wedge but heat transfer in both. Again, when the flow is bounded by rigid surfaces or

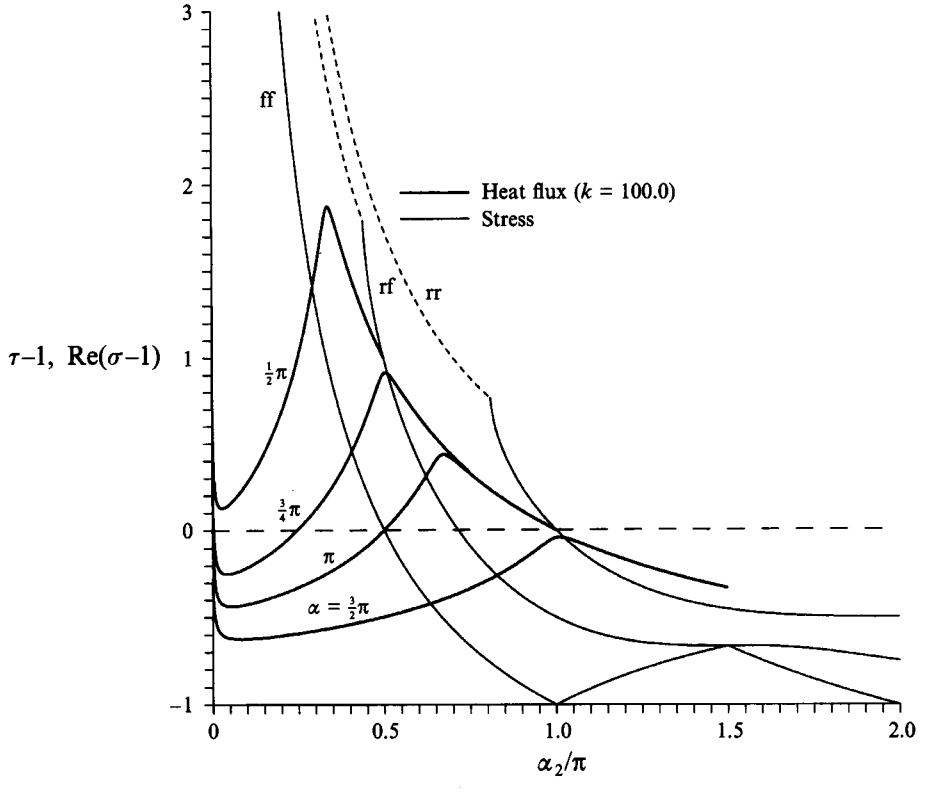

FIGURE 10. Two-phase non-isothermal flow: a comparison of the heat-flux and stress exponents for two-phase heat transfer for Case 1 and single-phase flow. The heat-flux results shown are for $k = 100.0$ and total wedge angles $\alpha = \frac{1}{2}\pi, \frac{3}{4}\pi, \pi$, and $\frac{3}{2}\pi$. Note that α_2 cannot exceed α. We see that the flux is more singular for small values of α_2 while the stress may be more singular for larger values of α_2. When thermocapillary effects are included, we expect solvability conditions at the points where the stress and heat-flux exponents intersect.

by isothermal boundaries, or when $\gamma' = 0$ there is no coupling. In these cases the solutions to the non-isothermal flow problem are just the single-phase isothermal flow solution and the two-phase thermal field solution. We can compare the heat-flux and stress exponents in these cases to determine which field has the stronger singularity. This comparison allows one to determine which singularity places stronger resolution requirements on a numerical simulation, for example.

Figure 10 shows heat-flux exponents for the thermal fields in Case 1 for conductivity ratio $k = 100.0$ and the real part of the stress exponents for the rigid/rigid wedge (Dean & Montagnon 1949), the rigid/free wedge (Moffatt 1964), and the free/free wedge (Moffatt 1964; Anderson & Davis 1993) for several values of the total wedge angle, α. Note that α_2 cannot exceed α. The heat flux tends to be the stronger field for small values of the wedge angle α_2 (the wedge containing the liquid). For larger values of α_2 either field can be stronger, depending on α and k. Note that the right-hand portions of the curves, $\tau - 1$, are bounded by $\tau = (\pi/\alpha) - 1$. We recognize this boundary as the heat-flux exponent for the thermal field in a single wedge for the nf/nf case.

Figure 11 shows a similar plot for the thermal fields in Case 2 with $k = 0.01$. Again, for small values of α_2 the heat flux is the stronger field. For larger values of α_2 either field can be stronger. The right-hand portions of the curves, $\tau - 1$, are bounded by $\tau = (\pi/2\alpha) - 1$, which we recognize as the heat-flux exponent for the thermal field in a

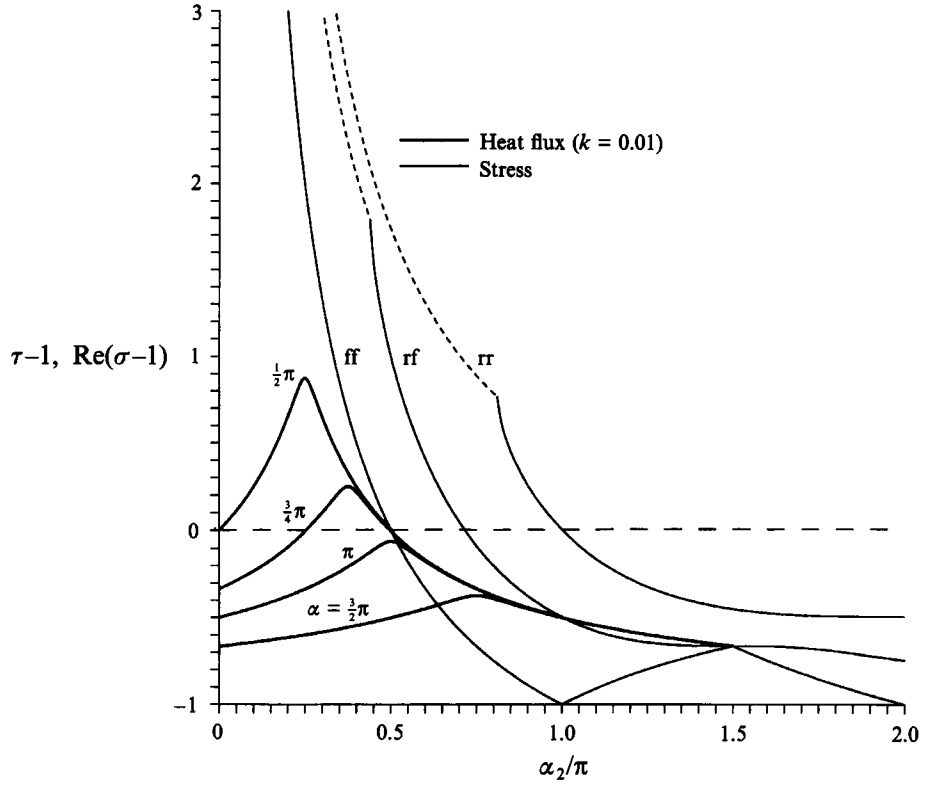

FIGURE 11. Two-phase non-isothermal flow: a comparison of the heat-flux and stress exponents for two-phase heat transfer for Case 2 and single-phase flow. The heat-flux results shown are for $k = 0.01$ and total wedge angles $\alpha = \frac{1}{2}\pi$, $\frac{3}{4}\pi$, π, and $\frac{3}{2}\pi$. Note that α_2 cannot exceed α. For larger values of k the heat-flux exponent is smaller, indicating an even more singular heat flux. When thermocapillary effects are included, we expect solvability conditions at the points where the stress and heat-flux exponents intersect.

Hydrodynamic b.c.		Thermal b.c.		
$\theta = 0$	$\theta = \alpha_2$	$\theta = -\alpha_1$	$\theta = 0$	$\theta = \alpha_2$
rigid	free	nf	continuity	nf
rigid	free	ft	continuity	nf
free	free	nf	continuity	nf
free	free	ft	continuity	nf

TABLE 4. Types of boundary conditions for two-phase non-isothermal flow

single wedge for the ft/nf case. Also note that the results shown here are for small k; the heat flux becomes more singular as k increases (see figure 7). Therefore, for a rigid/rigid liquid wedge the heat flux always has the stronger singularity, for a rigid/free liquid wedge the heat flux is always stronger for $\alpha < \pi$, and for a free/free liquid wedge the heat flux is always stronger for $\alpha < \frac{1}{2}\pi$.

The boundary conditions for the cases that allow thermocapillary coupling are listed in table 4. As in the single-phase non-isothermal flow problems we find that the thermal fields decouple from the flow and can be determined in advance of the flow field.

Therefore the thermal-field results are just the two-phase thermal-field results of §3.1 (see equations (3.2)–(3.7)). For the flow, since we are considering just a single liquid phase the general formulae found for the streamfunction in §2.2.1 still apply. The values of τ and $f_\tau(\theta)$ in these formulae correspond to thermal field, T_2 of §3.1.

Rigid/free wedge, no-flux/continuity/no-flux: Here we have thermocapillarity on the free surface $\theta = \alpha_2$. The thermal fields are given by (3.2) and (3.3). The streamfunctions are given by the expressions in §2.2.1 for cases (1i)–(2ii). As in the single-phase analysis we have solvability problems that arise when the forcing term is resonant. These resonant cases can be most easily recognized as the points where the solutions of (3.3) intersect the solutions of

$$\tau \sin 2\alpha_2 - \sin 2\tau\alpha_2 = 0. \tag{3.17}$$

Examples of such intersections can be seen in figure 10. In such a case, the forcing is resonant, and solutions to the coupled system exist only when $\alpha_2 = \pi$ and $\tau = 2, 3, 4, \ldots$. That is, solutions exist only when the intersections occur at these values. For partial local solutions the exponents τ and σ are those shown in figure 10.

Local solutions exist for $\alpha_2 = \pi$. The value of τ is determined by (3.3) with $\alpha_2 = \pi$. Thus, any solution, $\tau = \tau(\alpha, k)$ such that $\alpha > \pi$ and $\alpha_2 = \pi$ is a valid local solution.

Michael (1958) found that a *stress-free* planar free surface and a planar rigid boundary must meet at an angle of π. In comparison with this result we note that the flow in our case corresponds to zero normal stress but *non-zero* shear stress due to thermocapillarity on the free surface. However, we still find that a non-isothermal planar free surface upon which $\gamma' \neq 0$ must be oriented at an angle of π in order to satisfy all local boundary conditions.

Rigid/free, fixed-temperature/continuity/no-flux: Here the results are analogous to the previous case. The thermal fields are given by (3.4) and (3.5). Again, solvability problems are present in the resonant cases where τ and α_2 satisfy simultaneously (3.5) and (3.17). There are examples of these intersections in figure 11. No solutions to the coupled problem exist unless $\alpha_2 = \pi$ and $\tau = 2, 3, 4, \ldots$. The flow for partial local solutions is given by the general non-isothermal flow results of §2.2.1 where τ and $f_\tau(\theta)$ are determined by (3.4) and (3.5).

The flow for local solutions is given by the general non-isothermal flow results of §2.2.1 where $f_\tau(\theta)$ is given by (3.4) with $\alpha_2 = \pi$ and τ determined by (3.5).

Free/free, no-flux/continuity/no-flux: Thermocapillary effects are present on both $\theta = 0$ and $\theta = \alpha_2$. The phase between $\theta = 0$ and $\theta = -\alpha_1$ can be thought of as a heat-conducting medium with no flow.

Partial local solutions are given by the expressions in §2.2.1 with τ and $f_\tau(\theta)$ given by (3.2) and (3.3). Values of τ and σ appearing in these streamfunctions are shown in figure 10.

The conditions required for local solutions given by (2.29) with α replaced by α_2 and (3.3), which determines τ, can only be satisfied when $\alpha_2 = \pi$. Therefore, the local solutions for general values of τ such that $\sin(\tau \pm 1)\alpha_2 \neq 0$ have streamfunctions given by (2.28) where τ and $f_\tau(\theta)$ are given by (3.2) and (3.3) with $\alpha_2 = \pi$. When $\alpha_2 = \pi$ and $\tau = 1, 2, 3, \ldots$ solvability requires that $\gamma'_0 = \gamma'_\alpha$ and the streamfunction is given by (2.33) with $\alpha_1 = j\pi/\tau$, $j = 1, 2, 3, \ldots, \tau$, and $f_\tau(0) = A^{th}(-1)^j$.

Free/free, fixed-temperature/continuity/no-flux: This case is analogous to the previous case. The only difference is that the boundary $\theta = -\alpha_1$ is at a fixed temperature. Thermocapillary effects are still present on both $\theta = 0$ and $\theta = \alpha_2$.

Partial local solutions are given by the expressions in §2.2.1 with τ and $f_\tau(\theta)$ given by (3.4) and (3.5). Values of τ and σ appearing in these streamfunctions are shown in figure 11.

The conditions required for local solutions given by (2.29) and (3.5), which determine τ, can again only be satisfied when $\alpha_2 = \pi$. Therefore, the local solutions for general values of τ such that $\sin(\tau \pm 1)\alpha_2 \neq 0$ have streamfunctions given by (2.28) where τ and $f_\tau(\theta)$ are given by (3.4) and (3.5) with $\alpha_2 = \pi$. When $\alpha_2 = \pi$ and $\tau = 1, 2, 3, \ldots$ solvability requires that $\gamma_0' = \gamma_\alpha'$ and the streamfunction is given by (2.33) with $\alpha_1 = (j+\frac{1}{2})\pi/\tau$, $j = 0, 1, 2, \ldots, \tau$, and $f_\tau(0) = A^{th}(-1)^\tau$.

4. Small-capillary-number expansion

In this section we shall extend the small-capillary-number analysis of Anderson & Davis (1993) to non-isothermal flow. While there are several possible cases which can be analysed here, for demonstration purposes we shall consider the case of a solid/liquid double wedge with thermal boundary conditions corresponding to Case 2 in §3.1 (the second of table 4). However, the free surface is not assumed to be planar; we take $\alpha_2 = \alpha_2(r)$.

We expand

$$\psi = \tilde{\psi} + C\psi_1 + \ldots, \tag{4.1a}$$

$$\alpha_2 = \alpha_2^{(0)} + C\alpha_2^{(1)} + C^2\alpha_2^{(2)} + \ldots, \tag{4.1b}$$

$$T_i = T_i^{(0)} + CT_i^{(1)} + \ldots \tag{4.1c}$$

for $i = 1, 2$. The streamfunction satisfies the biharmonic equation and is subject to the boundary conditions (2.19*a–c*) and the normal-stress boundary condition

$$C[\boldsymbol{\sigma}\cdot\hat{\boldsymbol{n}}]\cdot\hat{\boldsymbol{n}} = -\nabla\cdot\hat{\boldsymbol{n}} \quad \text{on} \quad \theta = \alpha_2(r). \tag{4.2}$$

The thermal fields satisfy the conditions given in §3.1 for Case 2. Note that since α_2 is no longer independent of r, the boundary conditions become more complicated.

At leading order, the normal-stress boundary condition is satisfied by taking $\alpha_2^{(0)}$ constant. Therefore, the leading-order streamfunction, $\tilde{\psi}$, is just a partial local solution such as given in §2.2. Note that both isothermal and non-isothermal contributions are of interest here. The leading-order thermal field is given by (3.4) where τ is determined by (3.5).

Of particular interest is the free-surface position. From the normal-stress boundary condition we can obtain the $O(C^2)$ term for $\alpha_2^{(0)}$ with flow and thermal-field corrections up to $O(C)$. If we include higher orders, we find that

$$\alpha_2 = \alpha_2^{(0)} + C\{F_0 r^\sigma + G_0 r^\tau\} + C^2\{F_1 r^{2\sigma} + G_1 r^{2\tau}\} + \ldots. \tag{4.3}$$

This contains the isothermal (F_0 and F_1) and the non-isothermal (G_0 and G_1) contributions. The streamfunction and temperature corrections terms are of the form $\psi_1 = f_1(\theta) r^{2\sigma+1} + g_1(\theta) r^{2\tau+1}$, and $T_i^{(1)} = B_i(\theta) r^{2\tau}$ for $i = 1, 2$. The coefficients in (4.3) are given by

$$F_0 = -\frac{4\sigma}{(\sigma+1)} \frac{D_\sigma \sin\alpha_2^{(0)}}{\sin\sigma\alpha_2^{(0)}}, \tag{4.4a}$$

$$F_1 = -\frac{32\sigma D_\sigma^2[\sigma^2(\sigma^2-1)\sin^4\alpha_2^{(0)} + (\sin 2\sigma\alpha_2^{(0)} - 1)(\sigma^2\sin^2\alpha_2^{(0)} - \sin^2\sigma\alpha_2^{(0)})]}{(\sigma+1)^2\sin^2\sigma\alpha_2^{(0)}(2\sigma\sin 2\alpha_2^{(0)} - \sin 4\sigma\alpha_2^{(0)})}, \tag{4.4b}$$

$$G_0 = \frac{2\tau\gamma' A^{th}\sin^2\alpha_2^{(0)}}{\mu(\tau\sin 2\alpha_2^{(0)} - \sin 2\tau\alpha_2^{(0)})}, \tag{4.4c}$$

$$G_1 = -\frac{1}{2\tau(2\tau+1)}\left\{\frac{g_1''' + (2\tau+1)^2 g_1'}{2\tau-1} + 4\tau g_1' + G_0\left[\frac{g_0'''' + (\tau+1)^2 g_0''}{\tau-1} + 4\tau g_0''\right]\right\}, \tag{4.4d}$$

where σ satisfies $\sigma \sin 2\alpha_2^{(0)} - \sin 2\sigma\alpha_2^{(0)} = 0$, the derivatives of g_0 and g_1 are evaluated at $\theta = \alpha_2^{(0)}$, and we assume that $\tau \sin 2\alpha_2^{(0)} - \sin 2\tau\alpha_2^{(0)} \neq 0$. We note here that the zeros of F_0 and G_0 correspond to those angles, namely $\alpha_2^{(0)} = \pi$, that have zero normal stress on $\theta = \alpha_2^{(0)}$ and therefore correspond to the angles where local solutions exist.

Following Anderson & Davis (1993) we expand the value of α_2 in (4.3) for angles near π and find that

$$\alpha_2 = \alpha_2^{(0)} + C\{\tfrac{4}{3}D_{\frac{1}{2}}(\alpha_2^{(0)} - \pi)\, r^{\frac{1}{2}} + \tfrac{4}{3}D_2\, r^2 + J_0(\alpha_2^{(0)} - \pi)^2\, r^\tau + \ldots\} + C^2\left\{-\tfrac{32}{9}D_{\frac{1}{2}}^2 \frac{r}{\alpha_2^{(0)} - \pi} + J_1(\alpha_2^{(0)} - \pi)^2 r^{2\tau} + \ldots\right\} + \ldots, \quad (4.5)$$

where
$$J_0 = -\frac{2\tau\gamma' A^{th}}{\mu \sin 2\tau\pi}, \quad (4.6a)$$

$$J_1 = -\frac{1}{2\tau(2\tau+1)}\left\{\left(\frac{\tau A^{th}\gamma'}{\mu}\right)^2\left(\frac{2(3\tau+1)}{\sin 2\tau\pi} - \frac{2(2\tau+1)^2\cos 2\tau\pi}{\cos^2\tau\pi \sin 2\tau\pi}\right)\right\}. \quad (4.6b)$$

In their isothermal analysis, Anderson & Davis (1993) were able to identify non-uniformities in the small-capillary-number expansions by considering the limits $r \to 0$ and $\alpha_2^{(0)} \to \pi$. Depending on the order in which these limits are taken, different results are obtained. We now wish to determine how these results are altered by the presence of non-isothermal contributions.

First, take $r \to 0$ (before $\alpha_2^{(0)} \to \pi$). Here we obtain

$$\alpha_2 = \alpha_2^{(0)} + C\{\tfrac{4}{3}D_{\frac{1}{2}}(\alpha_2^{(0)} - \pi)\, r^{\frac{1}{2}} + (\alpha_2^{(0)} - \pi)^2 J_0\, r^\tau + \ldots\} + C^2\left\{-\tfrac{32}{9}D_{\frac{1}{2}}^2 \frac{r}{\alpha_2^{(0)} - \pi} + (\alpha_2^{(0)} - \pi)^2 J_1\, r^{2\tau} + \ldots\right\} + \ldots. \quad (4.7)$$

If $\tau > \frac{1}{2}$, the result is the same as the isothermal result, namely

$$\alpha_2 = \alpha_2^{(0)} + C\{\tfrac{4}{3}D_{\frac{1}{2}}(\alpha_2^{(0)} - \pi)\, r^{\frac{1}{2}} + \ldots\} + C^2\left\{-\tfrac{32}{9}D_{\frac{1}{2}}^2 \frac{r}{\alpha_2^{(0)} - \pi} + \ldots\right\} + \ldots. \quad (4.8)$$

This requires that $(\alpha_2^{(0)} - \pi) \gg C^{\frac{1}{2}} r^{\frac{1}{4}}$. This representation shows that the local solution has a free surface with infinite curvature at $r = 0$. If $\tau < \frac{1}{2}$, we get

$$\alpha_2 = \alpha_2^{(0)} + C\{(\alpha_2^{(0)} - \pi)^2 J_0\, r^\tau + \ldots\} + C^2\{(\alpha_2^{(0)} - \pi)^2 J_1\, r^{2\tau} + \ldots\} + \ldots. \quad (4.9)$$

This also gives an interface that has infinite curvature at $r = 0$. For this to be asymptotically valid, we need $1 \gg Cr^\tau$. This is clearly satisfied as $r \to 0$ and the requirement for asymptoticity does not depend on the value of the angle.

Next, let $\alpha_2^{(0)} \to \pi$ (before $r \to 0$). Here, the isothermal terms are the dominant terms. We find that

$$\alpha_2 = \pi + (\alpha_2^{(0)} - \pi) + C\{\tfrac{4}{3}D_2\, r^2 + \ldots\} + C^2\left\{-\tfrac{32}{9}D_{\frac{1}{2}}^2 \frac{r}{\alpha_2^{(0)} - \pi} + \ldots\right\} + \ldots. \quad (4.10)$$

This corresponds to a planar free surface. This expansion is valid when $r \gg C/(\alpha_2^{(0)} - \pi)$. So $r \to 0$ is not allowed unless $C = 0$. Consequently, in this limit the expansion cannot be considered local and the non-isothermal terms do not change the expansion from the isothermal case.

In the isothermal case, Anderson & Davis (1993) concluded that a small-capillary-number analysis has non-uniformities as $r \to 0$ and $\alpha_2^{(0)} \to \pi$. In the non-isothermal case,

there again exist the same type of non-uniformities, the form of which is slightly different when $\tau < \frac{1}{2}$. This analysis, as in the isothermal case, also demonstrates the significance of partial local solutions.

5. Interpretations

Our intention here is to provide interpretations for the non-isothermal flow cases in which separable solutions with bounded temperatures and velocities of the forms (2.5) and (2.11) do not exist. In the single-phase non-isothermal flow analysis this 'non-existence' arose in the following cases: (r/f, nf/nf for $\alpha = \frac{1}{2}\pi, \frac{3}{2}\pi$), (r/f, ft/nf for $\alpha = \pi$), and (f/f, ft/nf for $\alpha = \frac{1}{2}\pi, \frac{3}{2}\pi$). For two-phase non-isothermal flow in a solid/liquid wedge this non-existence arose for more general wedge angles, depending on the conductivity ratio, k. We shall discuss in detail the first two single-phase cases and identify means by which solutions can be found.

First consider the single-phase case of a rigid/free wedge with no-flux/no-flux boundary conditions with wedge angle $\frac{1}{2}\pi$. Here we found that temperature distributions that were bounded as $r \to 0$ had the form $T \sim r^{\tau} f(\theta)$ where $\tau = 2, 4, 6, \ldots$. These allowed no solution to the coupled flow problem. However, if we consider solutions with unbounded temperatures at the origin, specifically a logarithmic temperature distribution, coupled solutions to the flow problem can be found. In this case the temperature and flow fields are given by

$$T = D^{th} + b_0 \ln r, \tag{5.1a}$$

$$\tilde{\psi} = -\frac{\gamma'_\alpha}{2\mu} b_0 r\left(\sin\theta - \theta\cos\theta - \frac{2}{\pi}\theta\sin\theta\right) + \tilde{\psi}_I, \tag{5.1b}$$

where $\tilde{\psi}_I$ represents the isothermal contribution and is given in Anderson & Davis (1993) by their equation (2.28). Note that the linear term in r is the dominant one near the corner. Logarithmic temperature distributions represent either heat sources or sinks at the wedge vertex. In the following analysis we show how these logarithmic temperature distributions are related to *two-phase* temperature distributions with bounded temperatures at $r = 0$.

Consider the two-phase problem with the double-wedge geometry where phase one is solid and phase two is liquid. For this example we take $\alpha_2 = \frac{1}{2}\pi$ and keep α_1 arbitrary but bounded away from zero. The key difference between this problem and the single-phase problem is the addition of an adjacent solid phase which conducts heat. For the thermal boundary conditions we consider those given as Case 2 of §3.1. In the limit $k \to \infty$ these boundary conditions approach the no-flux/no-flux boundary conditions in the liquid wedge.

The hydrodynamic boundary conditions are given by (2.19*a–c*) where $\alpha = \frac{1}{2}\pi$ (note that we are considering just partial local solutions). Solutions to this non-isothermal flow problem can be found. The thermal fields and corresponding values of τ are given by (3.4) and (3.5) and the streamfunction is given by

$$\tilde{\psi} = \frac{\gamma'_\alpha}{2\mu} A^{th} r^{\tau+1}\left[\frac{\tau}{\sin\tau\alpha_2}\sin\tau\theta\sin\theta + \frac{1}{\cos\tau\alpha_2}(\sin\tau\theta\cos\theta - \tau\cos\tau\theta\sin\theta)\right] + \tilde{\psi}_I, \tag{5.2}$$

where $\tilde{\psi}_I$ is given by (2.28) in Anderson & Davis (1993).

In the limit $k \to \infty$ we see that the smallest value of τ is given approximately by (3.11), or in this case,

$$\tau \sim (2/\pi\alpha_1 k)^{\frac{1}{2}}. \tag{5.3}$$

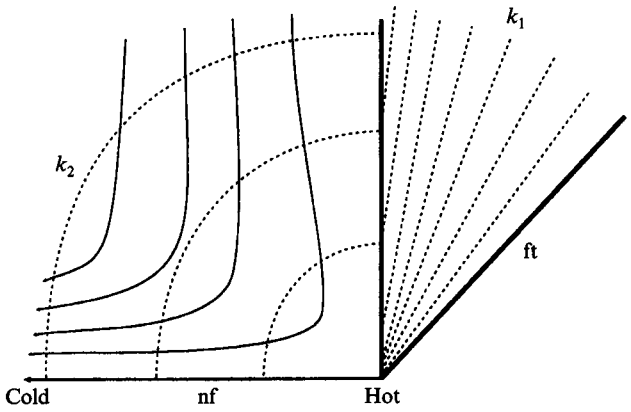

FIGURE 12. Two-phase non-isothermal flow, partial local solutions: a sketch of the streamlines (solid curves) and isotherms (dashed curves) corresponding to thermal boundary conditions in Case 2 with $k \gg 1$. Here there is fluid flow in phase 2 (i.e. phase 1 is solid) and heat transfer in both phases. The leading-order thermal fields are linear in θ (phase 1) and logarithmic in r (phase 2). The flow field is driven locally by thermocapillarity; the flow along the free surface is from hot to cold as indicated.

Note that this is the correct asymptotic form as $k \to \infty$ for values of α_1 bounded away from zero. Note also that $\sin \tau\alpha_2$ and $\cos \tau\alpha_2$ are non-vanishing for large but finite k. If we now fix r and let $\tau \to 0$ (i.e. $k \to \infty$) in the expressions for the thermal fields and streamfunction we find that

$$T_1 = T_{\alpha_1} + A^{th}[1 + \theta/\alpha_1], \tag{5.4a}$$

$$T_2 = T_{\alpha_1} + A^{th}[1 + \tau \ln r] \tag{5.4b}$$

and

$$\tilde{\psi} = \tilde{\psi}_I - (\gamma'_\alpha/2\mu)\tau A^{th} r[\sin\theta - \theta\cos\theta - (2/\pi)\theta\sin\theta]. \tag{5.4c}$$

Taking $D^{th} = T_{\alpha_1} + A^{th}$ and $b_0 = \tau A^{th}$ gives the previous single-phase result for T_2 in (5.1). Figure 12 shows the streamlines (solid curves) and isotherms (dashed curves) for the two-phase problem in this limit.

Note that this result was derived for general values of α_1 and holds as long as α_1 is bounded away from zero. We obtain similar results for the single-phase case with the same boundary conditions where the wedge angle is $\frac{3}{2}\pi$.

This shows that for the two-phase problem with $k \to \infty$, most of the heat is conducted through the corner; in the single-phase limit this is represented by a heat source or a heat sink at the corner. Keller (1987) encountered a similar situation when considering the conductance of a material in a corner region defined by an array of blocks where adjacent blocks had high/low conductivities.

There are several comments to be made about these results. We found that the limit $k \to \infty$ is non-uniform as $r \to 0$ for the temperature field but uniform for the flow. This shows that the logarithmic temperature distribution, which is 'necessary' in the single-phase analysis, is actually the result of a limiting case of a 'regular' temperature distribution in the two-phase problem. The assumption that the two-phase problem can be described by a single phase with bounded temperatures breaks down because the limit $k \to \infty$ and $r \to 0$ is non-uniform. This example shows that single-phase models with separable solution forms may be too idealized in certain cases.

Next consider partial local solutions for the case of flow in a single phase bounded by a rigid surface and a free surface with wedge angle π; the rigid boundary has a fixed-temperature condition and the free surface is a no-flux boundary. We shall relate this to a soluble problem in a two-phase medium with heat transfer and fluid flow in both phases.

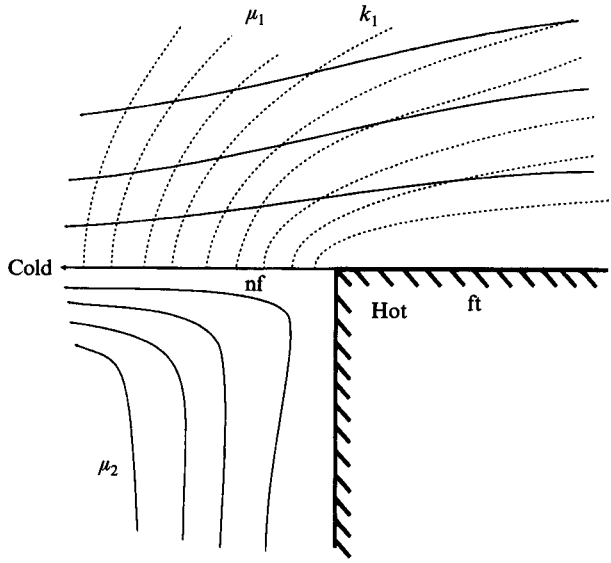

FIGURE 13. Two-phase non-isothermal flow, partial local solutions: a sketch of the streamlines (solid curves) and isotherms (dashed curves) with two fluid phases and just one thermal phase (i.e. $k_2 = 0$). The flow in phase 2 is driven directly by thermocapillarity. The flow in phase 1 has zero shear stress on $\theta = 0$ but is driven by viscous drag due to the motion in phase 2. Thermocapillarity drives the flow outward from hot to cold along the free surface separating the two fluid phases. The existence of a solution for $k = 0$ when fluids on *both* sides of the free surface are included indicates that the interactions from the second phase, even one with relatively small viscosity, are important.

Consider the general two-phase problem which has heat transfer and fluid flow in both wedges for the case where $\alpha_1 = \pi$ and $\alpha_2 = \frac{1}{2}\pi$. The boundaries $\theta = -\alpha_1$ and $\theta = \alpha_2$ will be taken to be rigid and isothermal (each at the same fixed temperature); however, for the purposes of the discussion here, the choice of boundary condition on $\theta = \alpha_2$ is not critical. We can address the single-phase problem by looking at the heat transfer and fluid flow in phase 1 in the limit $k = k_2/k_1 \to 0$ and $\mu = \mu_2/\mu_1 \to 0$ where μ_1 and μ_2 are the viscosities in fluids 1 and 2, respectively.

The hydrodynamic boundary conditions are discussed in the Appendix. A key difference between the two-fluid and the single-fluid cases is that here the *jump* in the shear stresses balances the surface-tension gradients. The non-isothermal flow problem can be solved for general values of k and μ in this case and we find that, in general, thermocapillary effects drive a flow in both phases (see the Appendix). As both $k \to 0$ and $\mu \to 0$, the denominator in the streamfunction approaches zero and in the case $k = \mu = 0$ the form of the solution becomes invalid, revealing the same 'non-existence' problems as found in the single-phase analysis. However, as long as either k or μ is non-zero the streamfunction representation is valid.

Suppose that we take $k = 0$ and allow heat transfer in phase 1 only. Here we find that $\partial^2\psi_1/\partial\theta^2 = 0$ on $\theta = 0$ so the shear stress boundary condition (A 1) is effectively reduced to

$$\frac{\partial^2\psi_2}{\partial\theta^2} = \tau\frac{\gamma_0'}{\mu_2} f_\tau(0)\, r^{\tau+1}. \tag{5.5}$$

This shows tht thermocapillarity necessarily drives a flow in phase 2. Since for partial local solutions the viscosity enters only through the shear-stress boundary condition, this indicates that the flow which is still present in *both* phases, is independent of the viscosity in phase 1. When $k = 0$, the effect of taking $\mu_2 = 0$ is that thermocapillarity

cannot drive a flow in *either* phase. In the limit of $\mu_2 \to 0$ the streamfunction becomes unbounded unless $\gamma_0' f_\tau(0) \to 0$ which suggests that the thermocapillarity must be weak. However, as noted by Proudman & Asadullah (1988), a Stokes flow description requires that the viscosity is not vanishingly small. Therefore we must let $\mu \to 0$ by taking $\mu_1 \to \infty$ while keeping μ_2 finite; then we find a valid solution which has flow in both phases. Figure 13 shows a sketch of the streamlines and isotherms in this case. The flow in phase 2 is driven directly by thermocapillarity; here the flow is driven towards the colder region, away from the corner. The flow in phase 1 is not directly driven by thermocapillarity (it has zero shear stress on $\theta = 0$) but motion in that phase is induced from the flow in phase 2 through viscous drag acting through the no-slip condition. Therefore we still see flow in two phases. The isotherms shown correspond to a single-phase heat transfer problem. This analysis suggests that the reason why the single-phase model is not sufficient in this case is that thermocapillarity necessarily drives a flow in the second phase.

Now suppose that we take $\mu_2 = 0$. This gives fluid flow in phase 1 only. In order to obtain a solution in this case, we must have non-zero conductivity, and hence heat transfer, in the second phase. Mathematically, the existence of non-zero conductivity in the second phase changes the value of the exponent, τ. Depending on the thermal boundary condition applied on the boundary $\theta = \alpha_2 = \frac{1}{2}\pi$, the smallest value of τ (which is $\frac{1}{2}$ when $k = 0$) either increases or decreases (for a no-flux condition τ decreases and for a fixed-temperature condition τ increases). Physically, the existence of non-zero conductivity in the second phase changes the temperature gradient, and hence the thermocapillary forcing on the free boundary.

These examples show that solvability problems in single-phase cases can be relieved by allowing fluid flow and/or heat transfer in an adjacent phase. We expect that similar ideas can be applied to the solvability cases which arose in the analysis of §3.2 where non-isothermal flow in a solid/liquid wedge was considered.

6. Summary

We have presented a local picture of fluid flow and heat transfer near contact lines. We have studied single- and multiple-phase systems with single and multiple fields. The class of solutions sought are those with bounded temperatures and velocities at the wedge vertex. Locally, the governing equations simplify to Laplace's equation and the biharmonic equation for the temperature and streamfunction, respectively. Separable solutions to the temperature and streamfunction are written as $T \sim r^\tau f_\tau(\theta)$ and $\psi \sim r^{\sigma+1} f_\sigma(\theta)$, respectively. For the streamfunction, we distinguish between local solutions, those that satisfy all local boundary conditions, and partial local solutions, those that satisfy all local boundary conditions except for the normal-stress boundary condition. The analysis provides locally valid solutions that identify the types of singularities that are present at the corner and show how these singularities vary with the wedge angle.

For single-phase heat transfer the temperature exponent, τ, is inversely proportional to the wedge angle (see figure 1). The dominant contribution to the heat flux near the corner varies like $r^{\tau-1}$ except for the case with two isothermal boundaries (at two different temperatures) where the heat flux has an r^{-1} behaviour. In all cases the exponent, τ, is purely real, giving monotonic temperature distributions in radial distance from the corner.

For non-isothermal flow in a single phase there is no convective coupling in the local wedge region though the temperature and flow fields can be coupled through thermocapillarity along a non-isothermal free surface.

For rigid surfaces, isothermal free surfaces, or for cases where $\gamma' = |\mathrm{d}\gamma/\mathrm{d}T| = 0$, there is no local coupling between the thermal and flow fields. In these cases the flow is given by the isothermal-flow results while the thermal fields are given by the pure heat-transfer results. The heat flux and stress exponents, $\tau - 1$ and $\mathrm{Re}(\sigma - 1)$, are those shown in figures 2–4. From these plots, the field with the stronger singularity can be identified.

When non-isothermal free surfaces are present, the flow field may be coupled to the temperature field through thermocapillarity. We find that the thermal field decouples from the flow leaving $T \sim r^{\tau}$ as in the pure-thermal problems. The resulting mathematical system for the flow is inhomogeneous with driving terms proportional to the thermal gradients along the free surface. The resulting streamfunction then has particular terms proportional to $r^{\tau+1}$, which balance forces on the free surface, as well as homogeneous terms proportional to $r^{\sigma+1}$, which correspond to zero shear stress. Although it is the particular terms that balance the surface-tension gradients, either may be the locally dominant component of the flow depending on which exponent, $\mathrm{Re}(\sigma)$ or τ, is smaller (see figures 2–4).

For two-phase heat transfer we found that the temperature exponent, τ, depends on the geometry, the thermal conductivity ratio, k, as well as the conditions applied on the wedge boundaries. The exponent, τ, is always real-valued. Also, for fixed interior wedge ratios (i.e. fixed α_1/α_2) and fixed values of k, τ is inversely proportional to the total wedge angle. However, τ remains finite as either α_1 or $\alpha_2 \to 0$. Its specific dependence on the relative size of the interior angles varies with the type of thermal boundary conditions applied on the two outer-wedge boundaries (see figures 6–9). In an analogous fashion to Proudman & Asadullah (1988), we have identified two modes of heat flow when the conductivity ratio is large or small. The temperature mode corresponds to the mode predicted from the single-phase analysis and has $O(1)$ temperature on the boundary between the two phases. The heat flux mode is the mode not obtained from the single-phase analysis. Here the phase with the larger conductivity has relatively constant temperature and the phase with the smaller conductivity 'sees' the boundary between the two phases as a fixed-temperature boundary. We also observe root-splitting features for asymptotically large and small conductivity ratios similar to those discussed by Anderson & Davis (1993) for two-fluid flow in a wedge. We obtain values for the total wedge angle which give bounds on the regions in which the heat flux is singular. For no-flux conditions on the two outer boundaries, the heat flux is never singular for $\alpha \leqslant \frac{1}{2}\pi$ while it is always so for $\alpha \geqslant \frac{3}{2}\pi$. Between these values the wedge geometry and conductivity ratio determine whether or not the heat flux is singular. For the case with one outer boundary held at a fixed temperature and the other with a no-flux condition the heat flux is always singular for $\alpha \geqslant \pi$. For $\alpha < \pi$ the wedge geometry and conductivity ratio determine whether or not the heat flux is singular.

Non-isothermal flow in two phases is analogous to non-isothermal flow in a single phase. We considered fluid flow in a single wedge and heat transfer in two wedges with various boundary conditions. The form of the thermocapillary forcing is the same as in the single-phase problems; however, the specific values of the thermal gradients are different.

When only rigid surfaces or isothermal free surfaces are present, or when $\gamma' = |\mathrm{d}\gamma/\mathrm{d}T| = 0$, there is no local coupling of the temperature and flow fields. In these cases the flow is given by the single-phase isothermal flow results (see Anderson & Davis 1993) while the temperature is given by the two-phase pure-heat-transfer results. The strengths of the singularities in these fields can be compared (see figures 10 and 11).

When non-isothermal free surfaces are present with $\gamma' \neq 0$, the flow is driven in part by the local surface-tension gradients. The thermal fields again decouple from the flow and are given by the two-phase pure-heat-transfer results. For the flow problem we again find particular solutions with $r^{\tau+1}$ and homogeneous solutions with $r^{\sigma+1}$. Solvability problems arise when τ corresponds to an eigenvalue of the homogeneous flow problem. Although the thermal fields were found to be monotonic in r in all cases (i.e. τ is real-valued) this is consistent with the existence of Moffatt vortices because locally there is no convection. In this analysis we find that local solutions exist only for liquid wedge angles of π. This can be compared with Michael's local result for isothermal flow in a rigid/free wedge which requires a wedge angle of π in order to satisfy all local boundary conditions (Michael 1958). For the isothermal wedge there is zero normal *and* shear stress on the free surface. For the non-isothermal problem there is zero normal stress but non-zero shear stress due to surface-tension gradients.

We also analysed non-isothermal flow using a perturbation expansion for small capillary number. This is analogous to that of Anderson & Davis (1993) for isothermal flow, where they identified non-uniformities near the corner for liquid wedge angles near π and found that the interface has infinite curvature at $r = 0$. For non-isothermal flow in this limit, the valid local solution also corresponds to a free surface with infinite curvature at $r = 0$; this singularity is stronger when the heat-flux exponent is smaller than the stress exponent.

In the non-isothermal flow problems, when τ corresponds to an eigenvalue of the isothermal, or homogeneous, system the thermocapillary forcing is resonant, and solutions to the non-isothermal flow problem can be found only if certain solvability conditions are satisfied. For single-phase non-isothermal flow we encountered cases in which no solutions in the class of functions sought could be found. These were (i) (r/f, nf/nf for $\alpha = \frac{1}{2}\pi, \frac{3}{2}\pi$), (ii) (r/f, ft/nf for $\alpha = \pi$), and (iii) (f/f, ft/nf for $\alpha = \frac{1}{2}\pi, \frac{3}{2}\pi$). We found that case (i) could be resolved by considering a two-phase system with one solid and one liquid wedge. Here the limit of large conductivity in the liquid phase (i.e. $k \rightarrow \infty$) regains the single-phase wedge problem. In this case a 'regular' solution to the two-phase system gives a logarithmic temperature distribution in the liquid wedge for asymptotically large conductivity ratio, k (i.e. the conductivity in the liquid phase much larger than that in the solid phase). This indicates that for large k most of the heat in the two-phase problem is conducted through the corner. This situation is represented by a heat source or sink in the single-wedge problem. For case (ii) we showed that solutions can be found when either a second fluid phase, a second heat conducting phase, or both are present. When there is heat conduction in the original phase only, thermocapillarity necessarily drives a flow in the second phase. When there is fluid flow in the original phase only, solutions can be obtained only when there is non-zero conductivity in the second phase. These observations show that under certain conditions single-phase models with simple separable solution forms are too special to depict the physics realistically.

This work was supported by grants from the National Aeronautics and Space Administration through the Graduate Student Researchers Program (D.M.A.) and the Program on Microgravity Science and Applications (S.H.D.). The authors would like to thank Dr D. A. Huntley for helpful discussions.

Appendix. Streamfunctions for non-isothermal two-fluid flow

The following shows the streamfunction for the non-isothermal fluid flow and heat transfer in which two liquid phases are present. We consider only partial local solutions for the double wedge with $\alpha_1 = \pi$, $\alpha_2 = \frac{1}{2}\pi$. The fluid viscosities are μ_1 and μ_2 for phases 1 and 2, respectively, and we define a viscosity ratio $\mu = \mu_2/\mu_1$.

The boundary conditions on the streamfunctions, ψ_1 and ψ_2, are those given in Anderson & Davis (1993, equations (3.1)) with their shear stress boundary condition (3.1*e*) replaced by

$$\mu\frac{\partial^2\psi_2}{\partial\theta^2} - \frac{\partial^2\psi_1}{\partial\theta^2} = \tau\frac{\gamma_0'}{\mu_1}f_\tau(0)\,r^{\tau+1} \quad \text{on} \quad \theta = 0. \tag{A 1}$$

The streamfunction form we seek is

$$\psi_i = r^{\tau+1}[A_\tau^{(i)}\cos(\tau+1)\theta + B_\tau^{(i)}\sin(\tau+1)\theta + C_\tau^{(i)}\cos(\tau-1)\theta + D_\tau^{(i)}\sin(\tau-1)\theta] \tag{A 2}$$

for $i = 1, 2$. The coefficients are given by

$$A_\tau^{(1)} = -C_\tau^{(1)} = \frac{\frac{1}{4}(\gamma_0'/\mu_1)f_\tau(0)\cos\tau\pi(\tau^2 - \sin^2\tau(\frac{1}{2}\pi))}{\cos\tau\pi(\tau^2 - \sin^2\frac{1}{2}\tau\pi) - \frac{1}{2}\mu\sin^2\tau\pi}, \tag{A 3a}$$

$$A_\tau^{(2)} = -C_\tau^{(2)} = \frac{\frac{1}{8}(\gamma_0'/\mu_1)f_\tau(0)\sin^2\tau\pi}{\cos\tau\pi(\tau^2 - \sin^2\frac{1}{2}\tau\pi) - \frac{1}{2}\mu\sin^2\tau\pi}, \tag{A 3b}$$

$$B_\tau^{(1)} = -D_\tau^{(1)} = \frac{-\frac{1}{4}(\gamma_0'/\mu_1)f_\tau(0)\sin\tau\pi(\tau^2 - \sin^2\tau(\frac{1}{2}\pi))}{\cos\tau\pi(\tau^2 - \sin^2\frac{1}{2}\tau\pi) - \frac{1}{2}\mu\sin^2\tau\pi}, \tag{A 3c}$$

$$B_\tau^{(2)} = \frac{-\frac{1}{4}(\gamma_0'/\mu_1)f_\tau(0)\sin\tau\pi(\tau - \sin^2\tau(\frac{1}{2}\pi))}{\cos\tau\pi(\tau^2 - \sin^2\frac{1}{2}\tau\pi) - \frac{1}{2}\mu\sin^2\tau\pi}, \tag{A 3d}$$

$$D_\tau^{(2)} = \frac{-\frac{1}{4}(\gamma_0'/\mu_1)f_\tau(0)\sin\tau\pi(\tau + \sin^2\tau(\frac{1}{2}\pi))}{\cos\tau\pi(\tau^2 - \sin^2\frac{1}{2}\tau\pi) - \frac{1}{2}\mu\sin^2\tau\pi}, \tag{A 3e}$$

where τ is determined by

$$\sin\tfrac{3}{2}\tau\pi = (1-k)\sin\tau\pi\cos\tau(\tfrac{1}{2}\pi) \tag{A 4}$$

(i.e. Case 3 in §3.1 with both $\theta = -\pi$ and $\theta = \frac{1}{2}\pi$ at the same fixed temperature). Note that in the limit $k \to 0$ we find $\tau \sim \frac{1}{2}, \frac{3}{2}, \frac{5}{2}, \ldots$ or $\tau \sim 2, 4, 6, \ldots$. We can identify the fractional exponents corresponding to the temperature mode (where there is non-constant temperature on the interface $\theta = 0$) and the even exponents corresponding to the heat flux mode (where the interface $\theta = 0$ is essentially isothermal).

REFERENCES

ANDERSON, D. M. 1993 Corner flows, heat transfer, and phase transformation. PhD thesis, Northwestern University, Evanston, IL.

ANDERSON, D. M. & DAVIS, S. H. 1993 Two-fluid viscous flow in a corner. *J. Fluid Mech.* **257**, 1–31.

BROWN, R. A. 1988 Theory of transport processes in single crystal growth from the melt. *AIChE J.* **34**, 881–911.

BURGGRAF, O. R. 1966 Analytical and numerical studies of the structure of steady separated flows. *J. Fluid Mech.* **24**, 113–151.

DEAN, W. R. & MONTAGNON, P. E. 1949 On the steady motion of viscous liquid in a corner. *Proc. Camb. Phil. Soc.* **45**, 389–394.

EHRHARD, P. & DAVIS, S. H. 1991 Non-isothermal spreading of liquid drops on horizontal plates. *J. Fluid Mech.* **229**, 365–388.

KELLER, J. B. 1987 Effective conductivity of periodic composites composed of two very unequal conductors. *J. Math. Phys.* **28**, 2516–2520.

MICHAEL, D. H. 1958 The separation of a viscous liquid at a straight edge. *Mathematika* **5**, 82–84.

MOFFATT, H. K. 1964 Viscous and resistive eddies near a sharp corner. *J. Fluid Mech.* **18**, 1–18.

PROUDMAN, I. & ASADULLAH, M. 1988 Steady viscous flow near a stationary contact line. *J. Fluid Mech.* **187**, 35–43.

ZEBIB, A., HOMSY, G. M. & MEIBURG, E. 1985 High Marangoni number convection in a square cavity. *Phys. Fluids* **28**, 3467–3476.